8-2002

Heat Release Analysis and Modeling for a Common-Rail Diesel Engine

M. Rajkumar
University of Tennessee - Knoxville

To the Graduate Council:

I am submitting herewith a thesis written by M. Rajkumar entitled "Heat Release Analysis and Modeling for a Common-Rail Diesel Engine." I have examined the final electronic copy of this thesis for form and content and recommend that it be accepted in partial fulfillment of the requirements for the degree of Master of Science, with a major in Mechanical Engineering.

Dr. Ming Zheng, Major Professor

We have read this thesis and recommend its acceptance:

Dr. Jeffrey W. Hodgson, Dr. David K. Irick

Accepted for the Council:
Dixie L. Thompson

Vice Provost and Dean of the Graduate School

(Original signatures are on file with official student records.)

To the Graduate Council:

I am submitting herewith a thesis written by M.Rajkumar entitled "Heat Release Analysis and Modeling for a Common-Rail Diesel Engine". I have examined the final electronic copy of this thesis for form and content and recommend that it be accepted in partial fulfillment of the requirements for the degree of Master of Science, with a major in Mechanical Engineering.

Dr. Ming Zheng

We have read this thesis and
recommend its acceptance:

Dr. Jeffrey W. Hodgson

Dr. David K. Irick

Accepted for the Council:

Dr. Anne Mayhew

Vice Provost and Dean of
Graduate Studies

(Original signatures are on file with official student records.)

HEAT-RELEASE ANALYSIS AND MODELING FOR A COMMON-RAIL DIESEL ENGINE

A Thesis

Presented for the

Master of Science Degree

The University of Tennessee, Knoxville

M.Rajkumar

August 2002

Dedication

This dissertation is dedicated to my parents, Mr.M.Muthurajan and Mrs.M.Nagaratinam my sister, M.Uma Maheshwari and brother M.Anand, who are my great role models and friends, and for always believing in me, inspiring me, and encouraging me to reach higher in order to achieve my goals.

ACKNOWLEDGEMENTS

I take this opportunity to thank everyone who helped in completing my MS. I am extremely thankful to advisor Dr.Ming Zheng for his valuable guidance. Dr.Zheng extended his support in all areas of research: theoretical, data-acquisition and experimentation. I want to thank Dr.David.K.Irick and Mr.Daniel P.Graham for their valuable technical support in setting up the test rig. Mr. Dennis W. Higdon helped with the Electrical and Electronics part of this project and I am thankful to him. I am also thankful to Dr.Alberto Funioli who donated valuable equipments for conducting this research. I am thankful to Dr. Al Kornhauser of Virginia Tech for allowing me use his MATLAB programs for the analysis. I would also like to thank Dr.J.W.Hodgson for agreeing to be part of my committee.

Finally, I thank my friend Mr.M.Saravanan with whom I had numerous discussions, about this research.

ABSTRACT

The main purpose of this study was to perform a heat release analysis in order to formulate a heat-release model for a common-rail diesel engine. The fundamental idea of the model is to describe the observed physical processes with empirical formulas based on the experimental data.

A Fiat 2.4Liter common rail engine was used in the tests. A rotary incremental encoder with 0.1° resolution was coupled to the crankshaft pulley with a special adapter. The engine was operated at a number of different speeds and load conditions. Cylinder pressure data was recorded using a high-speed data acquisition system. The data acquisition was done at variable sampling speeds; encoder signal at every 0.1° dictated the sampling speed for data-acquisition. Cylinder pressure data was logged for 100 cycles at each operating condition. This raw data was averaged and used for further analysis. The actual rate of heat-release/crank angle was evaluated using the first law of thermodynamics. The heat release data was modeled using Weibe functions. Two such functions were used: one to describe the pilot burning and the other to describe the main burning stage of the combustion process. The coefficients and parameters in the model were adjusted to match the observed heat release diagram. Actual cylinder pressure versus crank angle traces were compared with predicted cylinder pressure versus crank angle traces for verification of the technique.

TABLE OF CONTENTS

CHAPTER **Page**

LIST OF FIGURES

Figure **Page**

Figure **Page**

LIST OF TABLES

NOMENCLATURE

NOx	Oxides of Nitrogen
PM	Particulate Matter
DI	Direct-Injection
IDI	Indirect Injection
TDC	Top Dead Center
BDC	Bottom Dead Center
CA	Crank Angle
SOI	Start of Injection
EOI	End of Injection
COV	Coefficient of Variance
IMEP	Indicated Mean Effective Pressure
EGR	Exhaust Gas Recirculation
γ	Ratio of Specific Heats

CHAPTER I
INTRODUCTION

1.1 Brief History of Diesel Engine

In 1892, German Engineer Rudolf Diesel proposed in his patent the concept of a compression-ignition engine [1]. He suggested that combustion might be initiated by injecting liquid fuel into air solely heated by compression. In his initial experiments, he injected coal dust into a cylinder containing air that had been compressed. Later on, he turned to liquid fuel and achieved success with what we now call diesel fuel.

Rudolf Diesel built and ran the first diesel engine at the Augsburg Maschinenfabrik (now known as MAN) in 1894 [2]. The single cylinder engine was used to power stationary machinery. The engine operated at 26.2% efficiency, a very significant improvement on the 20% achieved by the best gasoline engines of that time [1].

1.2 Fundamentals of Diesel Engine

As described by Heywood [3], diesel engines have been divided into two basic categories according to their combustion chamber design:

(1) Indirect injection (IDI) engines: In IDI engines the combustion chamber is divided into two regions, a pre-chamber and a main chamber. The fuel is injected into the “pre-chamber” which is connected to the main chamber via a passage or one or more orifices.

(2) Direct injection (DI) engines: DI engines have a single open combustion chamber into which fuel is directly injected.

1.2.1 Combustion in Diesel Engine

Combustion in diesel engines has been described in detail by Heywood [3]. According to Heywood, in a diesel engine air is compressed in the combustion chamber during the compression stroke, which greatly increases its temperature and pressure. In to this highly compressed and heated air, diesel fuel, which is at high pressure after compression in a fuel pump, is injected in the liquid state. The liquid fuel droplets absorb/extract heat from their surroundings and vaporize quickly. The temperature of the thin layer of air surrounding the droplet reduces but its temperature is again raised by heat transfer from the main bulk of air. As soon as this vapor and the adjacent air reach the auto-ignition temperature and the local air fuel ratio is within the combustible range, ignition takes place. Once ignition has taken place and flames are established, the thermal energy available for further evaporation is enhanced by that released by combustion. Thus, there is a delay period before ignition can take place. The initial fuel droplets meet air whose temperature is only a little above their self-ignition temperature and they ignite after ignition delay. The subsequent fuel droplets find air already heated to much higher temperatures by the burning of initial droplets and therefore their ignition delay is much shorter.

1.2.2 Stages of Combustion

The various stages of combustion as described by Heywood [3] are shown in Fig 1:

(1) First stage or the ignition delay period: This is the period between the start of fuel injection into the combustion chamber and the apparent start of combustion. This delay period is calculated by comparing the pressure diagrams of the fired and unfired cycle.

The point where the slope of the p-θ diagram of the fired cycle deviates from the unfired cycle is taken as the point where combustion begins. During this period, some fuel is added but not ignited. This is the short preparatory phase.

(2) Second stage or pre-mixed combustion phase: In this stage, combustion of the fuel that has mixed with air, is above self-ignition temperature, and has the required air/fuel ratio takes place during the first few degrees of crankshaft rotation. This stage is characterized by high heat release. About one-third of the heat is evolved during this period.

(3) Third stage or mixing-controlled combustion phase: Once the fuel and air that pre-mixed during the ignition delay have been consumed, the burning rate is controlled by the rate at which mixture becomes available for burning. The rate of burning is thus primarily dependent on the fuel vapor and air mixing process. The heat release rate reaches a lower peak in this phase and the rate decreases as the phase progresses. This stage is also called diffusion burning.

(4) Fourth stage or late combustion phase: Heat release continues at a lower rate during the expansion stroke. One of the possible reasons for heat release is that, some fuel energy is still present in soot and fuel-rich combustion products, and that fuel energy can be released. It's also possible that a small fraction of fuel is unburned. The final burnout process is slow because the temperature of the cylinder gases falls during expansion.

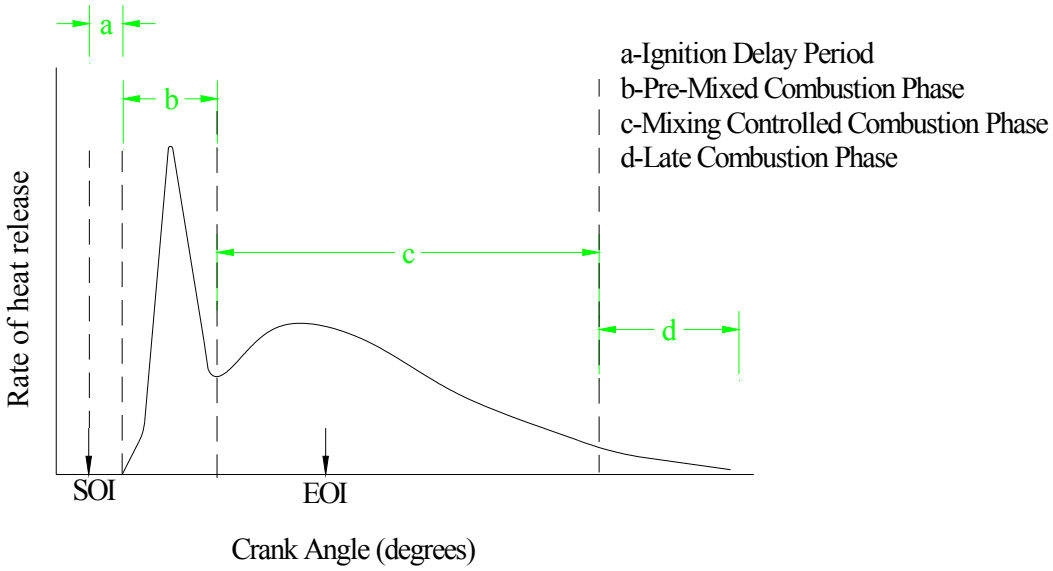

Figure 1. Typical DI Diesel Engine Heat Release Rate Diagram Identifying combustion phase [3]

1.2.3 Heat Release Analysis

W.T.Lyn [4] has described the combustion process as a link between the design and final aspects of engine performance in his pioneering research. According to Lyn, for a given engine specification, the performance of an engine is uniquely determined by the manner in which fuel is introduced into the combustion chamber, which in turn is determined by the design of the fuel injection equipment. Injection characteristics are defined by the following four items:

- Injection Timing
- Injection Period
- Shape of Injection Rate Diagram
- Spray Distribution
- Spray Droplet Size Distribution

The indicated efficiency for a given engine configuration is uniquely determined by the shape and magnitude of the cylinder pressure diagram, which in turn depends on the rate of heat release and heat transfer through the combustion chamber wall. Figure 2 shows the aspects of engine performance and the corresponding research area.

1.3 Common-Rail Engines

Common-rail engines are direct injection diesel engines with “Common-rail” fuel injection system. Common-rail engines use a common pressure accumulator called the rail and all the injectors are fed from this rail. Common-rail engines have the advantage of being able to control the injection pressure independent of the engine speed and load. Common-rail systems with electronically controlled fuel injection also have a provision

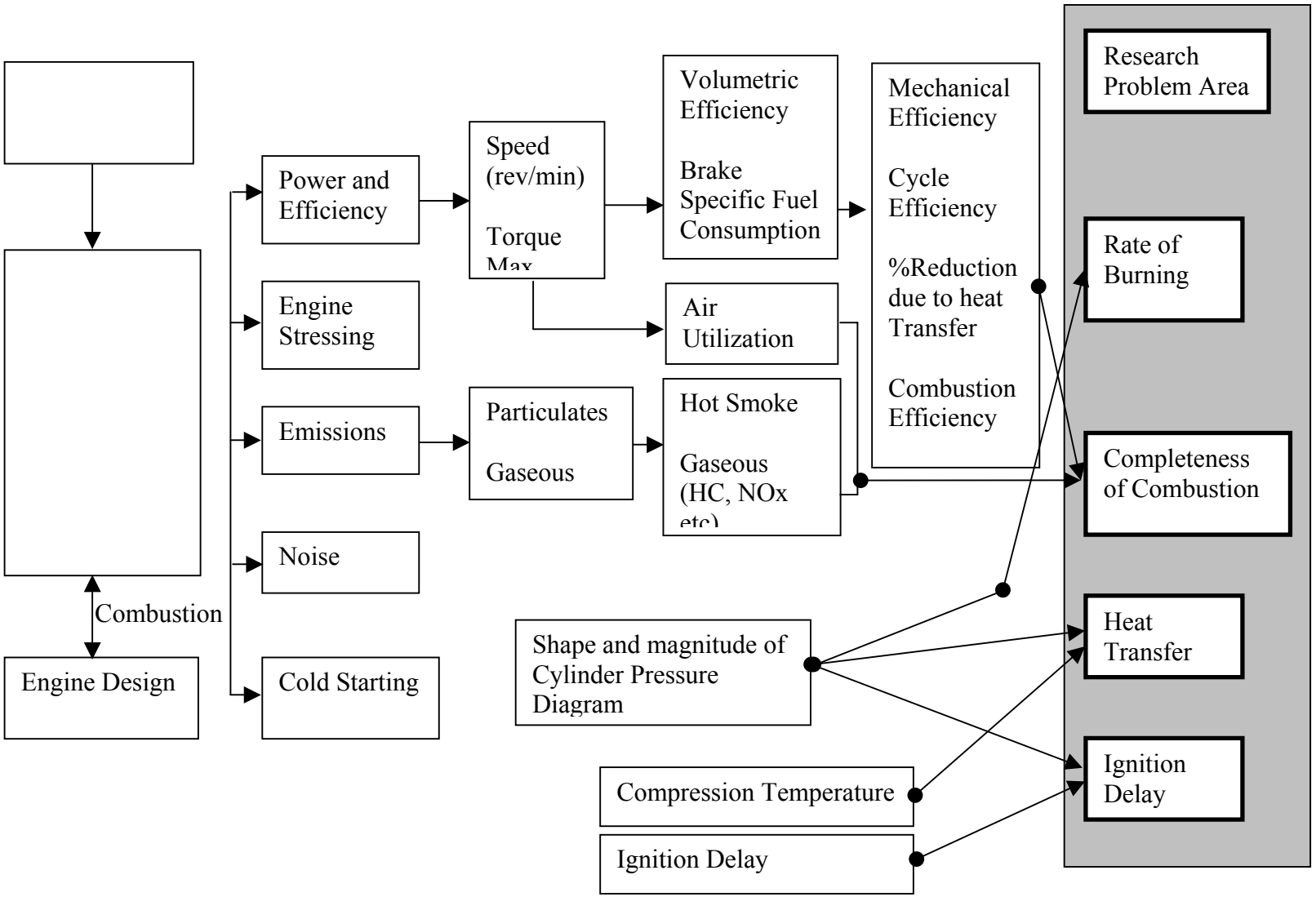

Figure 2. Aspects of Engine Performance [4]

for pilot injection, which has an important bearing on emissions.

Diesel engine researchers have always tried to come with up a flexible fuel-injection system that will allow control of:

- Start of injection
- Fuel quantity injected
- Injection pressure
- Injection shaping

In 1978, Bosch [5] came up with an electronically controlled accumulator injection system (Common Rail Injection System). This system was successful in meeting all the above stated goals.

The key elements of a common rail injection system are:

(a) High-pressure (controllable) pump

(b) Fuel rail with pressure sensor

(c) Electronically controlled injectors and

(d) Engine management system

Figure 3 shows the common rail set up for the Fiat engine used for experiments.

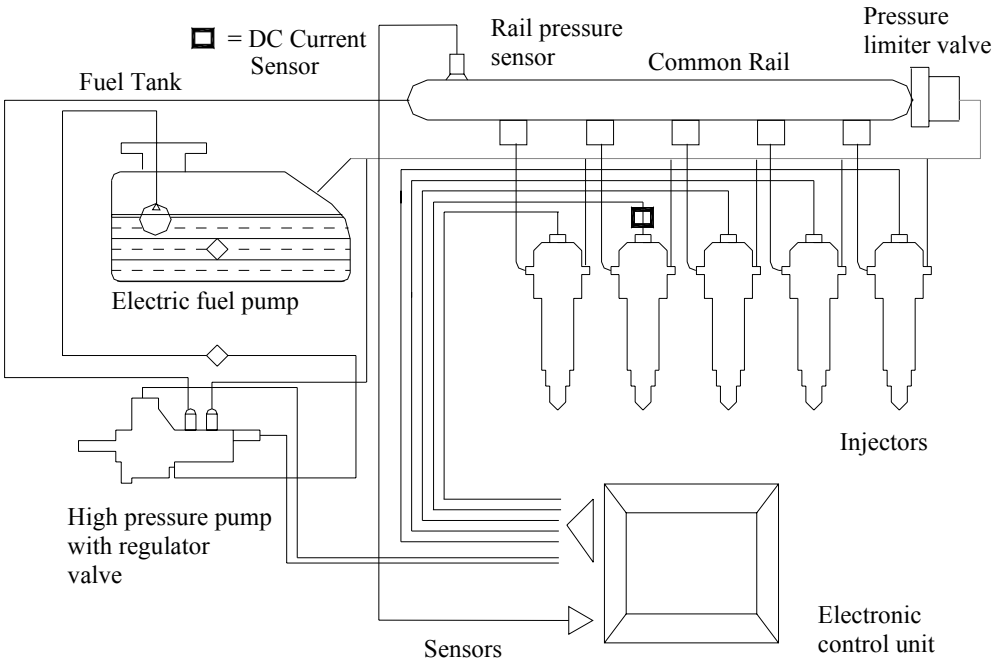

Figure 3. Common Rail Engines for Passenger Cars [6]

1.3.1 Operating Principle

As discussed by Stumpp and Ricco [6], in a common-rail engine, a feed pump delivers the fuel through a filter unit to the high-pressure pump. The high-pressure pump delivers fuel to the high-pressure accumulator (the rail). The injectors are fed from this rail. The injectors inject fuel into the combustion chamber when the solenoid valve is actuated. The fuel volume between the high-pressure pump and the injectors serves as an accumulator. This helps to dampen oscillations initiated by the pulsating delivery of the high-pressure pump. A pressure sensor measures the fuel pressure in the rail. Its value is compared to the desired value stored in the electronic control module (ECM). If the measured value is different from the desired value, an overflow orifice on the high-pressure side of the pressure regulator is opened or closed. The overflow fuel returns to the tank. The injector opening and closing is controlled by the ECM. The duration of injection, fuel pressure in the rail and the flow area of the injector determine the injected fuel quantity.

1.3.2 Components

The main components, as discussed by Stumpp and Ricco [6] are: high-pressure fuel pump, injector, accumulator, pressure sensor and ECM

a) High Pressure Pump

The high-pressure pump is usually a radial piston pump. The working of high pressure pump is shown in Figure 4. A cam on its drive shaft displaces three pistons in succession. The pistons are held to the eccentric by the springs and each piston draws fuel via a corresponding inlet valve. The drawn fuel is delivered via a check valve to the rail when

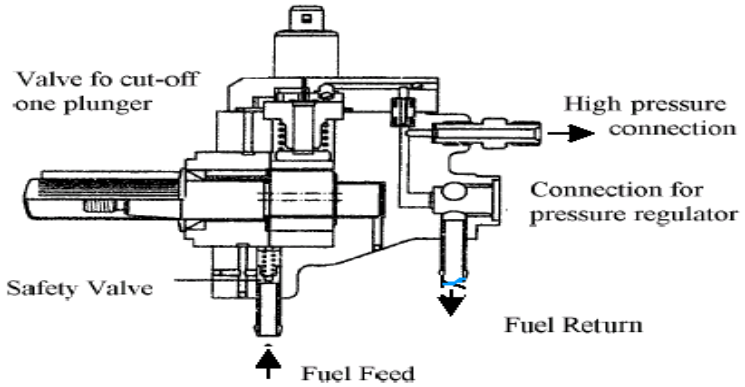

Figure 4. High-pressure fuel pump [6]

the piston is lifted The inlet valve of one piston can be opened by a solenoid. In this way, the quantity of the high-pressure fuel delivered can be matched to the demand.

A safety valve is also located in the fuel feed of the high-pressure pump. The piston of this valve closes an orifice in the inlet to the high-pressure pump when there is low fuel pressure. With high fuel pressure the orifice is open.

b) Injector

The injector consists of:

- A multi-hole nozzle with a spring, pressing the nozzle neddle to its sealing seat,
- A control piston P
- An orifice Z feeding fuel to the control piston
- An orifice A being opened or closed by a solenoid valve.

According to the authors, the deactivated solenoid valve closes the orifice A on the top of the control piston. The fuel pressure from the rail works on the top of the control piston via the throttle Z, thus the fuel pressure exerts a force in addition to the nozzle spring in

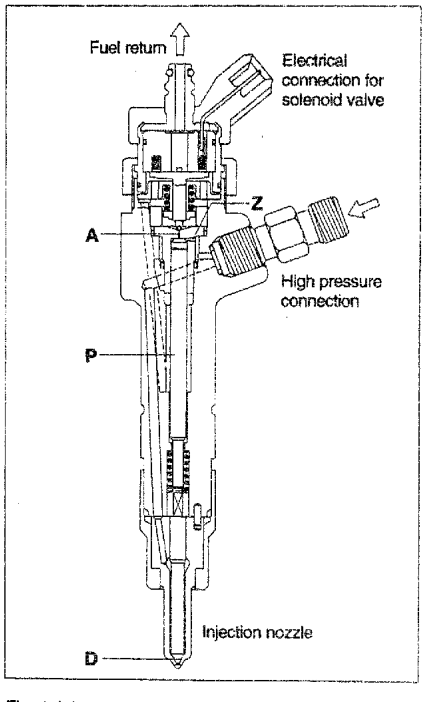

Figure 5. Injector [6]

closing the nozzle. When the solenoid is energized, the orifice A opens. This reduces the pressure on the control piston and the nozzle is opened. Afterwards when the solenoid valve is de-energized, the pressure exerted on the control piston raises and the injector closes. Figure 5 shows the details of the injector described.

c) Accumulator

The fuel trapped between the check valves in the high-pressure pump and the injector nozzle seat works as an accumulator. The trapped volume has an optimum value. A smaller volume results in large pulsations of fuel pressure whereas a larger volume increases the response time of the pressure during transient conditions.

d) Pressure Regulator

The pressure regulator varies the pressure in the accumulator. A solenoid acts as a ball overflow valve. Increasing current in the coil of the solenoid increases the solenoid force, raising the fuel pressure. The overflow fuel returns to the tank.

e) Electronic Control Unit (ECU)

The ECU controls all the important functions of the fuel injection system:

- Based on the engine operating conditions, the ECU evaluates the desired value of the fuel pressure. The ECU sends a signal to the pressure regulator if the desired fuel pressure is different from the measured fuel pressure.
- The solenoid valves of the injectors are controlled according to accelerator pedal position and operating information of the engine.
- The solenoid valve of the high-pressure pump is switched according to the engine operating information.
- The electric fuel pump is switched on/off by the ECM.

1.3.3 Advantages of Using Pilot Injection in Common Rail Engine

Pilot injection or pre-injection has been described by Manfred *et al* [8] as a means to optimize the emission behavior and reduce noise of direct injection diesel engines. According to the authors, the combustion process should have the following characteristics to achieve noise-free combustion with low exhaust emissions and they have divided the combustion process into three following phases:

Phase I: Beginning of Combustion—In this phase, only a small amount of fuel should be burnt to limit NOx and soot formation.

Phase II: Through end of Injection—Sufficient mixture of fuel and air should be available to reduce secondary soot formation.

Phase III: After end of injection—Intensified mixture of the residual air and the combustion gases in order to oxidize soot.

The authors found that pilot injection allows the diesel engine combustion in the above-mentioned way. The amount of fuel burnt in the first phase is lower in comparison to the conventional process since only pilot injection fuel is burnt in the beginning of the combustion. Pilot injection reduces the average combustion temperature due to reduced pre-mixed combustion and slower combustion during diffusion.

Soot formation is also effected by pilot injection. This was explained by examining the flame area fraction [9]. The author has shown that there is a direct relationship between flame area and smoke. If more pilot flame exists, when the main injection starts the interference of already formed soot with the main injection spray may cause poor mixing of the main spray and poor oxidization of the pilot combustion soot. The author also suggests optimizing pilot quantity and increasing the interval between the end of the pilot and the start of the main injection as a mean to reduce the flame area and hence the soot.

According to Manfred *et al* [8], the main reason for the reduction in combustion noise is the decrease of ignition delay due to the higher temperature at the start of the main injection. Long [9] has also explained this phenomenon in his paper. According to Long [9], longer ignition delays result in more mixture and stronger pre-mixed combustion if other conditions remain same. From this it can be clearly noted that pilot injection helps to shorten the ignition delay of the main injection and contributes to a reduction of

combustion noise by controlling the pre-mixed combustion. However, it should be noted that pilot injection has it's own ignition delay. Therefore, if the pilot quantity is too large the combustion noise of the pilot will become dominant.

1.3.4 Rail Pressure Maps

Cam driven injection systems build injection pressure for each injection. Thus, fuel metering and the pressure build-up are linked. The injection pressure results from the metered fuel quantity being pushed through the nozzle orifice by the injection piston with a velocity proportional to the engine speed.

However, in common rail systems fuel metering and pressure build-up are independent and the injection pressure is chosen as a function of engine parameters resulting in improved performance of the engine. Figure 6 shows the comparison of a conventional fuel injection system and a common rail injection system.

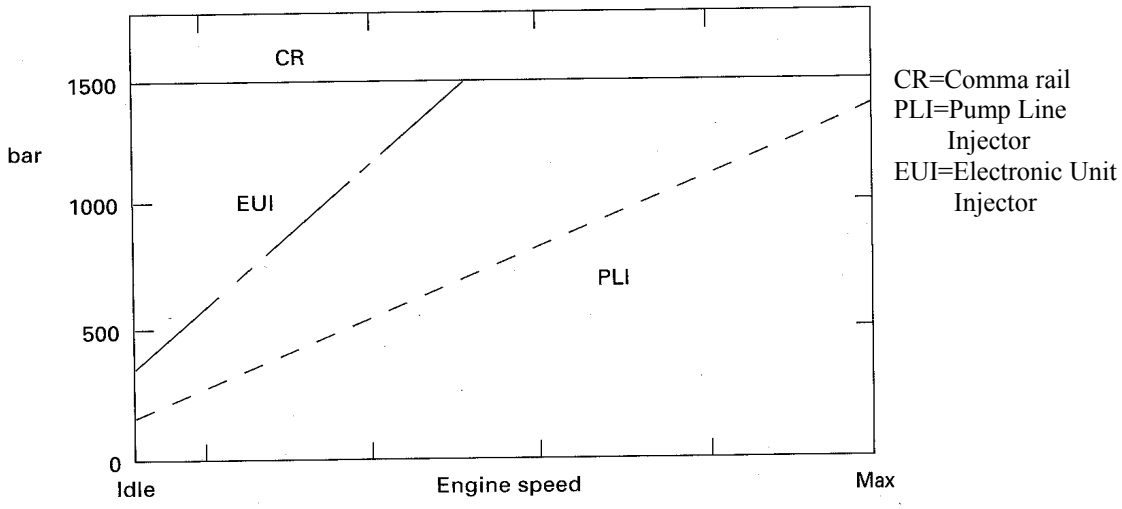

Figure 6. Rail Pressure variation with speeds in different Fuel Injection Systems [7]

The advantages and disadvantages of common rail and a conventional fuel injection system are listed in Table1.

Table 1. Comparison of Conventional and Common-Rail fuel injection system. [11]

Fuel injection System	**Advantages**	**Disadvantages**
Conventional	• Proven technology. • Variable injection Timing.	• Fuel injection pressure dependent on engine speed.
Common-Rail	• Variable injection timing. (pilot and main) • Fuel pressure independent of engine speed. • Constant fuel pressure at nozzle during injection period. • Post injection also possible • Good spray quality of fuel.	• Higher cost compared to the conventional system

CHAPTER II
EQUIPMENT

2.1 Engine Dynamometer

A water brake dynamometer (Manufacturer: Clayton Mfg Co Rating: 200HP at 2100rpm) was used to conduct the experiments. The output torque was displayed on an Omega model DP25-S strain gauge panel meter that displays the torque to ± 1ft-lb.

2.2 Cylinder Pressure Transducer

One glow plug was modified and used as an adapter for a cylinder pressure transducer. In this adapter, the pressure sensor was integrated into the shell of the glow-plug. The resulting package has identical displacement characteristics to the original plug and allows for direct pressure readings without cylinder head modifications in the engine.

An Optrand cylinder pressure sensor was used for cylinder pressure measurements. This sensor has been described in detail by Wlodarczyk Marek *et al* [13]. According to the author, the fiber optic sensor consists of three basic components: a sensing head directly exposed to combustion pressure, a fiber optic strand, and an opto-electronic module containing all the sensor's optical and electronic components.

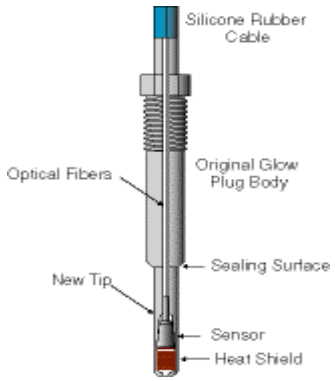

Figure 7. Cylinder Pressure Sensor [13].

Table 2. Cylinder Pressure Transducer Specifications [13]

SPECIFICATIONS:	
Pressure Range	0~200 bar
Temperature coefficient of sensitivity	+/-0.03%/°C
Output Signal	0.5~5V Analog

The sensor head consists of a metal housing with a welded sensing diaphragm, a fiber holding ferrule, and two fibers bonded inside the ferrule. The details of the sensor are shown in Figure 7. The sensing diaphragm is the most critical element of the sensor. It has to be as small as possible so that the embedded sensor occupies a very small amount of space in the device into which it is integrated. To ensure durable operation the present sensor uses a hat-shape diaphragm with varying thickness across its diameter. The diaphragm material is a high strength alloy (Inconel). The specifications of cylinder pressure transducer are shown in Table 2

2.3 Test Engine

All the tests were performed on a Fiat 2.4L. Refer to Table 3 for a complete description of the engine. For performing tests on this engine, the dynamometer cell was equipped with an external overflow cooling tower to provide adequate cooling for tests at high speed and high loads. A larger capacity intercooler was used. The cooling technique used was to keep the intercooler dipped in a water tank [12].

Table 3. Technical data for Fiat Engine (Fiat Technical Service Manual)

ALFA ROMEO DIESEL ENGINE		
Type		Diesel, 4 stroke
Cooling system		Water Cooled
Intake system		Turbocharged, inter-cooled, with un-cooled EGR
Fuel system		Bosch Radialjet Common Rail Fuel Injection
Displacement	Liter	2.387
Stroke	mm	90.4
Bore	mm	82
Connecting Rod Length	mm	150
Injection System		Common Rail System
Compression Ratio		18.45:1
Cylinder Configuration		In-Line
Number of Cylinders		5
Max Power		100kW @ 4200 RPM
Max Torque		304.2 Nm @ 2000RPM

2.4 Data Acquisition System

A high-speed portable Wavebook/516* model was used for data acquisition. The major characteristics of the system are:

- Up to 1-MHz sampling with 12 bit or 16-bit resolution, 8 differential inputs
- Single & multi-channel analog triggering with programmable level and slope
- Digital TTL-level and pattern triggering
- Pulse trigger
- External clock
- Eight or sixteen 1-MHz digital inputs

The data was logged on to a Pentium Pro desktop computer. Waveview* software that was provided as part of Wavebook* system was used for data acquisition. The sampling was done at a variable sampling rate using an external clock. The encoder signal (obtained every 0.1° CA) was used for deciding the sampling rate. The same signal was also used to trigger the sampling. Therefore, we have exactly one sample point corresponding to every 0.1° CA. The acquisition configuration (Figure 8,9 and 10) used for the data acquisition with the Wavebook* software is:

- Pre-trigger = 0
- Post-trigger = 720000 (100cycles)
- Rate = External (same as the 0.1° CA encoder signal)
- Triggering = Channel 1 Analog (same as the 0.1° CA encoder signal)

* Wavebook, Waveview, Wave book/516 are trademarks of IOTECH Inc.

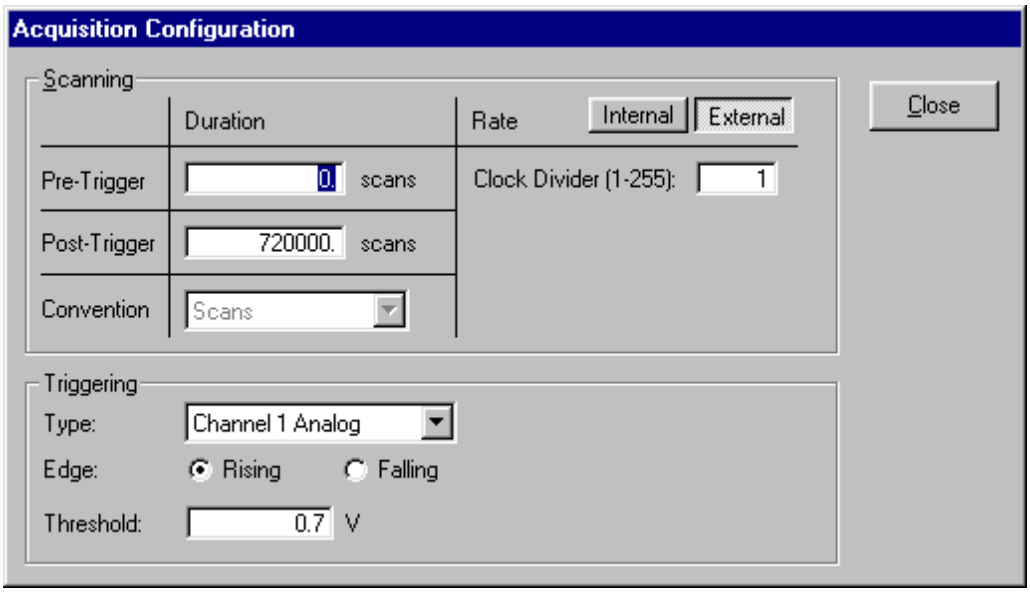

Figure 8. Acquisition Configuration Settings

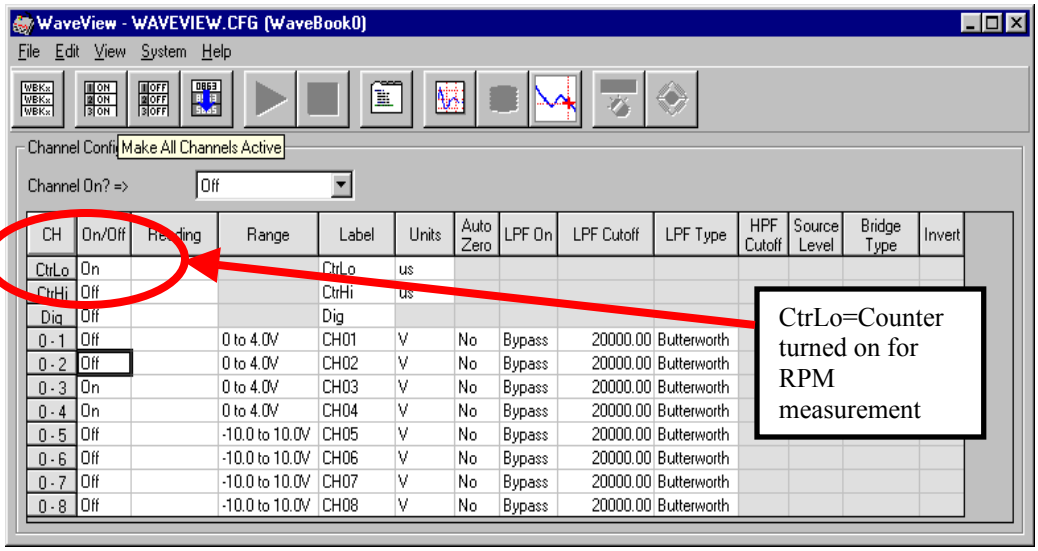

Figure 9. View of Configuration Sheet

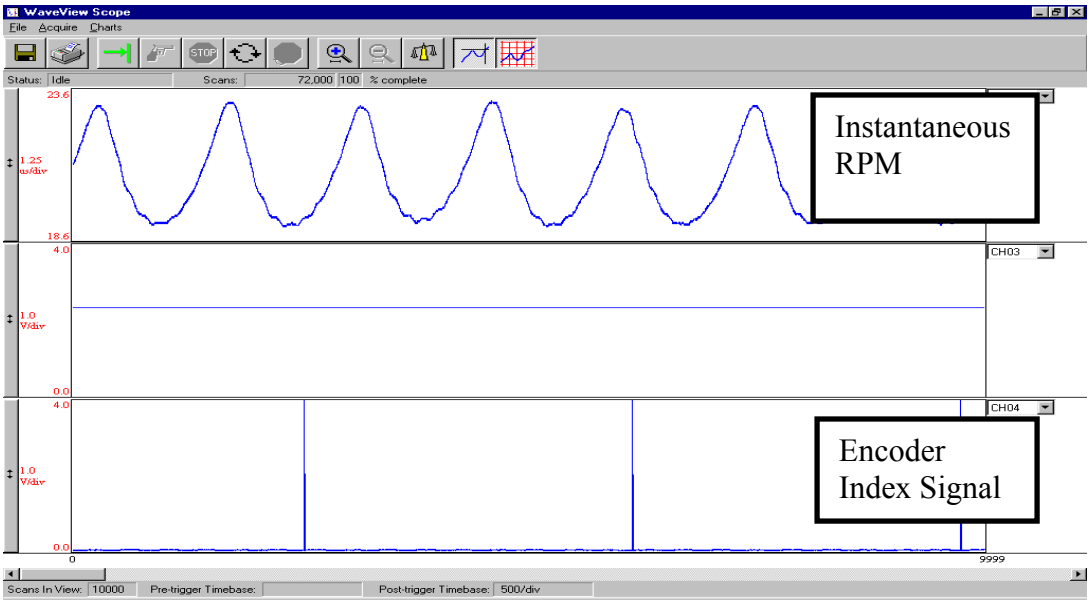

Figure 10. Screen Showing Instantaneous RPM and Encoder Index Signal

2.5 Crank-Angle Encoder

The engine crank angle position was accurately determined using a rotary incremental encoder (Manufacturer: Gurley Precision Instruments). It is important to understand each mechanical position is not uniquely defined in a rotary incremental encoder. Absolute encoders on the other hand have a unique value (voltage, binary count, etc) for each mechanical position.

Two output functions channel A and the index, from the encoder, were recorded along the cylinder pressure and fuel injection timing data. The encoder had a resolution of 0.1°. The crank angle resolution is defined as the crank angle interval at which the pressure data is measured. The main advantages of increasing the crank angle resolution are [14]:

1. The bandwidth is increased allowing a higher resolution of cylinder pressure variations to be obtained. This is especially useful in diesel engines, which have relatively high rates of pressure rise and heat release.

2. It increases the accuracy of identifying the crank angle position at which a certain absolute or rate of change of parameter occurs e.g. the crank angle position corresponding to the maximum cylinder pressure.

Increasing the crank angle resolution had additional advantage in this particular study because this allowed easier observation of the pilot injection. However, it is important to note that crank angle resolution is different from the calculation crank angle resolution. The calculation crank angle resolution is defined as the interval over which the calculation of the derived parameter like pressure rise rate and heat release rate is made. The calculation crank angle resolution for most parameters was 1° CA.

2.6 Fuel Injection Signal

The fuel injection signal was measured with a DC Current Sensor using the set-up as shown in Fig 11. Any rapid change in the injector current produces an induced emf. The DC Current sensor placed around the injector had a large number of turns which ensured that the induced output voltage is of the order of 0~1Volt.

The complete experimental setup is shown in Figure 12. The cylinder pressure sensor and DC current sensor were mounted on the first cylinder. The encoder was mounted on the crankshaft pulley using an adapter and a flexible coupling. Figure 13 shows the wiring diagram for the data acquisition system. 0.1° CA signal from the encoder goes to the external clock and the analog trigger thus ensuring that we have only one data point every 0.1° CA. Four signals; cylinder pressure, fuel injection, 0.1° CA and index signal were taken to the signal-conditioning unit. The data acquisition was done using Waview* software that accompanied the data-acquisition system.

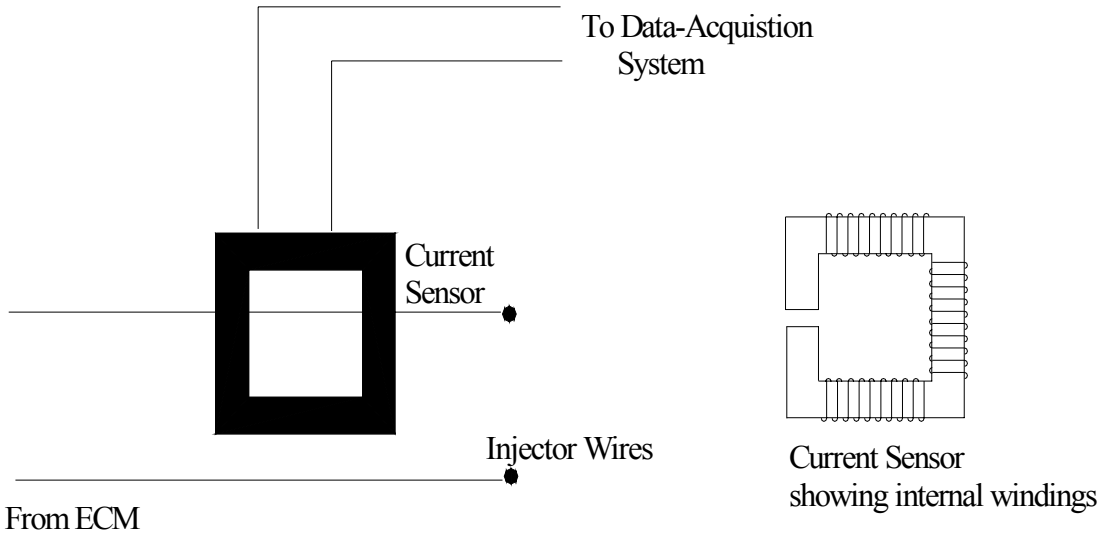

Figure 11. Principle for Fuel Injection Signal Measurement

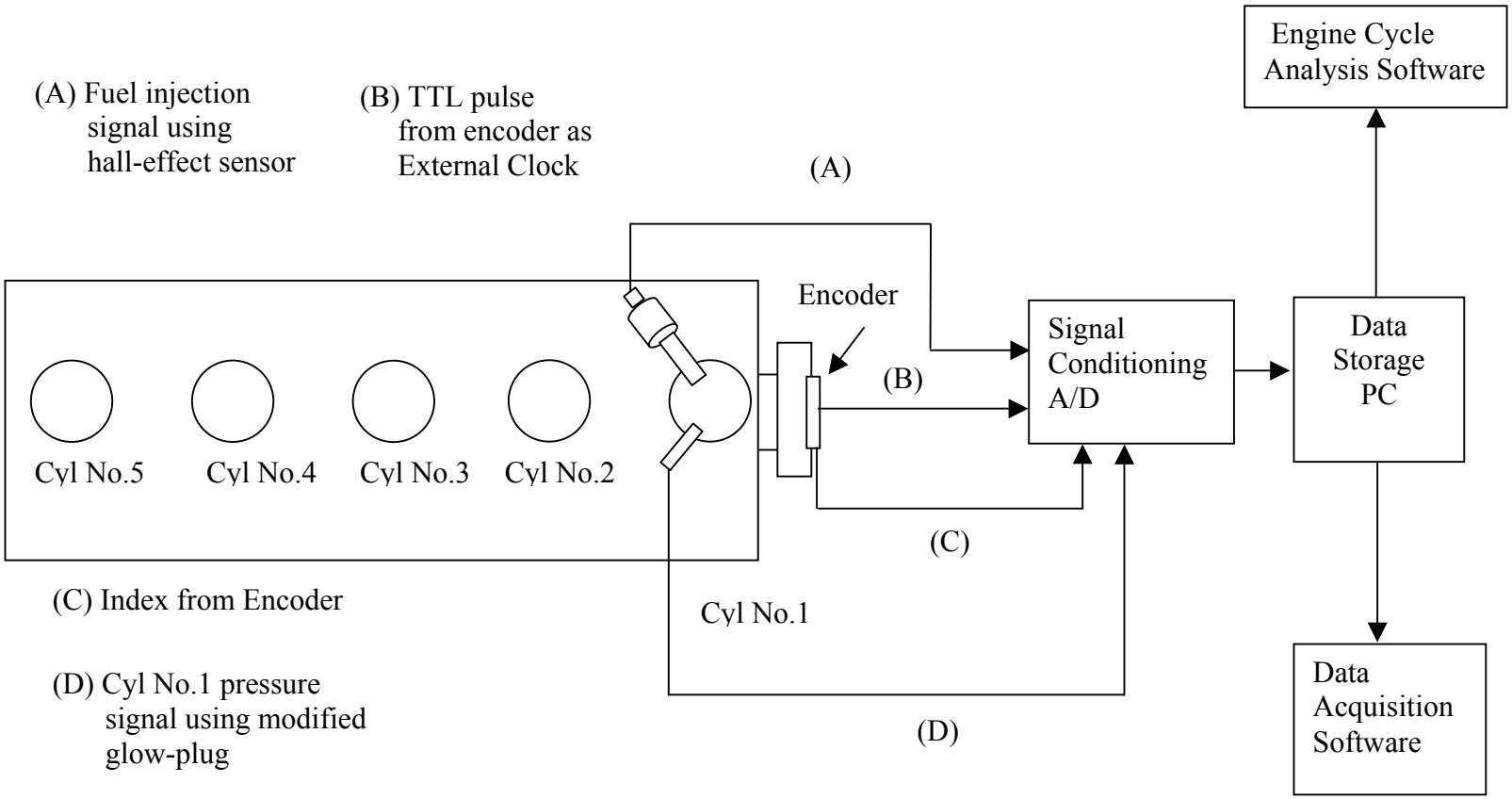

Figure 12. Experimental Setup

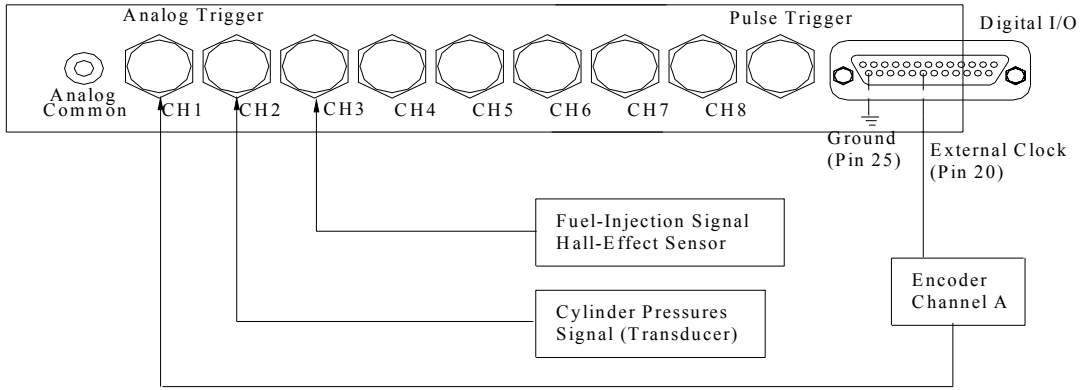

Figure 13. Schematic Diagram of WaveBook Assembly

CHAPTER III
PROCEDURE

3.1 Heat Release Analysis

In analyzing the combustion process, the principle diagnostic tool is the pressure versus crank angle curve. In addition to combustion, cylinder pressure is also affected by the changes in the volume of combustion chamber due to piston travel, heat transfer to the walls and blow-by. Therefore, in order to examine the combustion process it is necessary to relate each of the above to pressure rise and to separate the effect of combustion from the other effects. This type of data reduction is referred to as "Heat Release Analysis". This is done using the first law of thermodynamics.

The system of interest (shown in Figure 14) when analyzing the thermodynamics of combustion is the gas trapped in the combustion chamber during compression, combustion, and expansion process. The first law of thermodynamics for this system states

$$dU = \delta Q - \delta W \tag{3.1}$$

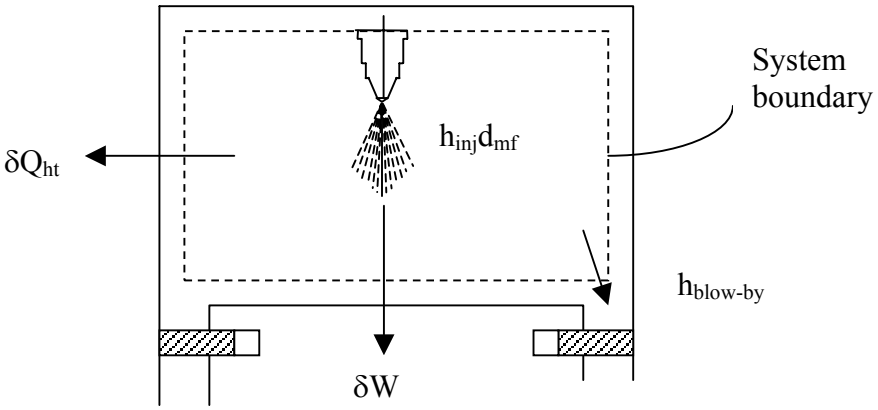

Figure 14. System boundary for combustion chamber for heat-release analysis

where, dU is the change in internal energy, δQ is the heat added to the system and δW is the mechanical work done by the system.

The internal energy of the gas in the combustion chamber can then be expressed using the molar specific internal energies according to (assuming complete combustion)

$$U = U(nC_xH_y, nO_2, nCO_2, nH_2O, nN_2, T) = \sum n_i \overline{u_i(T)} \tag{3.2}$$

$$dU = nC_v dT + \sum u_i dn_i \tag{3.3}$$

If the crevice effects are ignored and the gas composition inside the combustion chamber is assumed constant then applying ideal gas equation of state,

$$\delta Q = \frac{C_v}{R} d(pV) + pdV \tag{3.4}$$

Since crank-angle resolved measurements of p are already available, the above equation can be rewritten in crank angle dependent form

$$\frac{dQ}{d\alpha} = \frac{C_v}{R} \frac{d(pV)}{d\alpha} + p(\alpha) \frac{dV}{d\alpha} \tag{3.5}$$

The above equation can be integrated to give cumulative net heat release.

$$Q(\alpha) = \frac{C_v}{R} \left[p(\alpha)V(\alpha) - p(\alpha_0)V(\alpha_0) \right] + \int_{\alpha_0}^{\alpha} p(\alpha) \frac{dV}{d\alpha} d\alpha \tag{3.6}$$

This equation can be further simplified using finite sum instead of a continuous integral.

$$(Q)_i = \frac{C_v}{R} \left[p_i V_i - p_0 V_0 \right] + \sum_{j=0}^{i} p_j (\Delta V)_j \tag{3.7}$$

For the analysis, γ (ratio of specific heats) was assumed to be a function of temperature alone and is given by

$$\gamma = 1.35 - 6 \times 10^{-5} T + 1 \times 10^{-8} T^2 \quad (3.8)$$

Equation (3.7) was used as the final equation that is used to evaluate heat release at various crank-angles.

Heat Transfer Effects

Heat Transfer affects the engine performance, efficiency and emissions [3]. If the heat transfer to the combustion chamber walls increases, the average combustion gas temperature and pressure will decrease, and the work/cycle transferred to the piston will decrease. Thus, both specific power and the efficiency are affected by engine heat transfer.

The term Q_n denotes the net heat transfer across the system boundary (assuming heat that is released from the fuel crosses system boundary). It is the difference between the apparent gross heat-release rate and the heat transfer to the walls.

$$\frac{dQ_n}{dt} = \frac{dQ_{ch}}{dt} - \frac{dQ_{wall}}{dt} \quad (3.9)$$

where,

$\frac{dQ_n}{dt}$ = Apparent net heat release rate

$\frac{dQ_{ch}}{dt}$ = Apparent gross heat release rate

$\frac{dQ_{wall}}{dt}$ = Apparent rate of heat transfer to the walls

Heat transfer between the cylinder gases and the cylinder wall takes place during the entire engine cycle. During the intake and the early part of the compression stroke, heat is

transferred from the cylinder walls to the gases, but during the combustion and the expansion stroke heat is transferred from the gases to the cylinder wall.

The rate of heat transfer can be calculated as,

$$\frac{dQ_{wall}}{dt} = -Ah(T_w - T_{gas}) \tag{3.10}$$

The in-cylinder heat transfer coefficient varies with position and time. For the analysis, here only the variation with time/crank angle is considered as emissions are not being considered. The heat transfer to the wall has in general both a convective and a radiation component for diesel engines [3].

The heat-transfer coefficient can be estimated from Annand's [15] heat transfer correlation.

$$h = a\left(\frac{k}{B}\right)\mathrm{Re}^{0.7} + \frac{C}{\left(T - T_{wall}\right)}\left(T^4 - T_{wall}{}^4\right) \tag{3.11}$$

where,

B is the cylinder bore diameter in meters, T is the working fluid temperature in Kelvin, T_{wall} is the wall temperature in Kelvin, a is constant from 0.25~0.8 and $C = 0.576\sigma$ where $\sigma = 5.67 \times 10^{-8} Wm^{-2}K^{-4}$.

Re is the Reynolds number of the working fluid

$$\mathrm{Re} = \frac{Vd\rho}{\mu} \tag{3.12}$$

where,

V is the mean piston speed in meters per second, d is the bore diameter in meters, ρ is the density of the fluid in Kgm^{-3}, and μ is the dynamic fluid viscosity in $Kgm^{-1}s^{-1}$.

The mean piston speed is calculated from the engine speed

$$V = 2LN \tag{3.13}$$

where, N is the engine speed in revolutions per second and L = engine stroke in meters.

Annand [15] has approximated Prandtl Number as 0.7. Therefore,

$$k = \frac{Cp.\mu}{0.7} \quad \text{where } \mu = 4.702 \times 10^{-7}.T^{0.645} \tag{3.14}$$

$$Cp = \frac{R}{1-1/\gamma} \quad \text{where } \gamma = 1.35 - 6 \times 10^{-5} T + 1 \times 10^{-8} T^2 \tag{3.15}$$

3.2 Analysis of Cylinder Pressure Data

Cylinder pressure data were averaged over N cycles because average of N measurements is more reliable estimator of the average pressure at that crank angle than any individual cycle measurement [16]. Secondly, the engine itself is an averaging device, which responds to the mean values of air and fuel flows by generating mean indicated power. Therefore, it is appropriate to use the mean of many cycles. The number of consecutive cycles to be used for averaging is found by considering the variability inherent in the data and the accuracy required. To ensure with the confidence level of 99.9% that the sample mean was within 3% of population mean, sample average was based on 100 cycles. (Fig 34)

The following parameters were evaluated from the cylinder pressure plots:

1. P_{max} and the °CA(θ_{max}) corresponding to P_{max}
2. Rate of change of pressure versus °CA
3. IMEP of each cycle.
4. Work done during each cycle

5. Heat released versus °CA
6. Rate of heat released versus °CA
7. COV of IMEP (defines the cyclic variability in indicated work per cycle)

IMEP variation is studied as it directly influences drivability. According to Heywood, [3] an IMEP variation of more than 10% leads to poor drivability.

Engine cylinder pressure is a fundamental engine variable, necessary for nearly any type of engine and combustion analysis. As described earlier for a given engine, geometry the indicated efficiency is decided by the cylinder pressure trace [4]. Once we have a cylinder pressure trace, then the next thing evaluated is the rate of change of pressure and the peak pressure. This is so because combustion noise is directly related to rate of change of pressure and the peak cylinder pressure [17].

From the cylinder pressure data next step is to calculate the heat release characteristics. Engine designers have often tried to correlate performance variables such as brake specific particulates and NO to heat release rate. It has been suggested by John Abraham et al [18] that greater the proportion of heat released during the premix phase of diesel combustion, the greater the NO and the greater proportion of heat released during diffusion phase, the greater the particulates. A greater overall rate of heat release rate leads to lower particulates and greater NO and vice versa. Figures 15 to 30 show the cylinder pressure traces, rate of change of pressure and heat release characteristics for 1500 RPM and loads between 25% and 55%. Figure 31 and 32 give the details of calculated values of temperature and heat transfer coefficient at 1500 RPM and 25% load

Cylinder Pressure Data and Analysis: 1500 RPM and 25% load

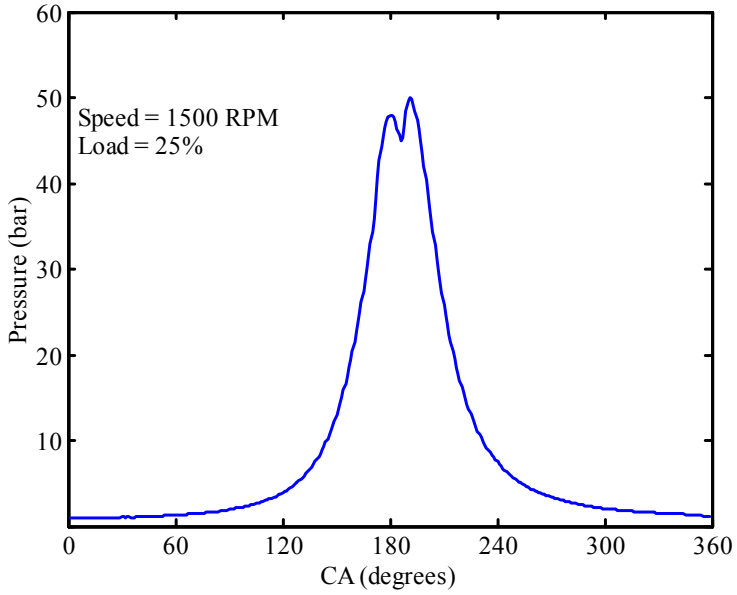

Figure 15. Averaged Smoothed Cylinder Pressure versus °CA (1500 RPM and 25% load)

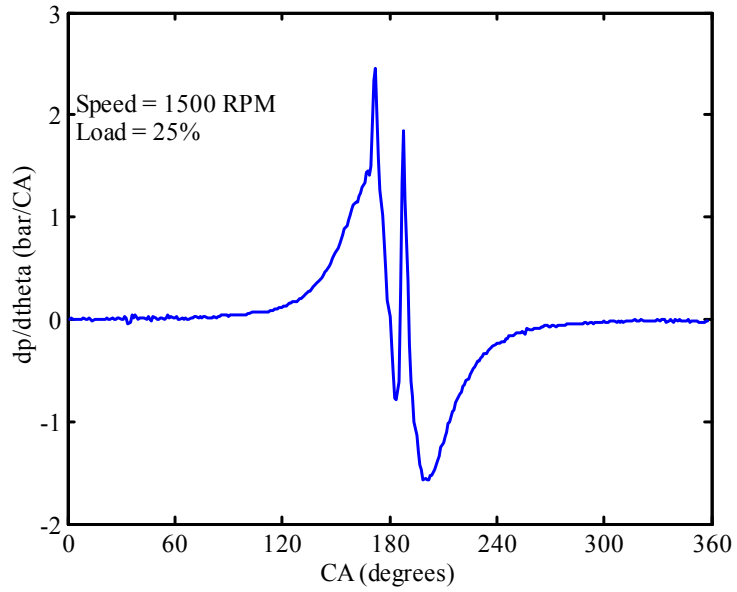

Figure 16. Rate of Change of Pressure versus °CA (1500 RPM and 25% load)

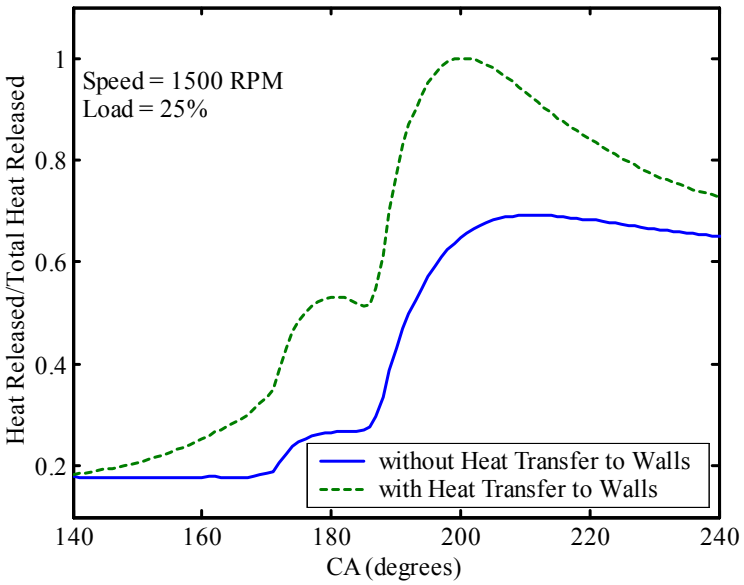

Figure 17. Normalized Heat Released versus °CA (1500 RPM and 25% load)

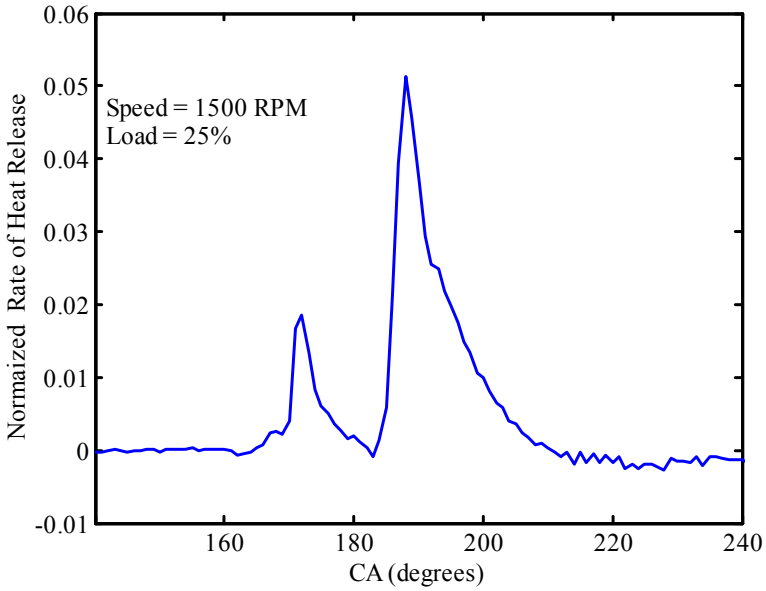

Figure 18. Normalized Rate of Heat Release versus °CA (1500 RPM and 25% load)

Cylinder Pressure Data and Analysis: 1500 RPM and 35% Load

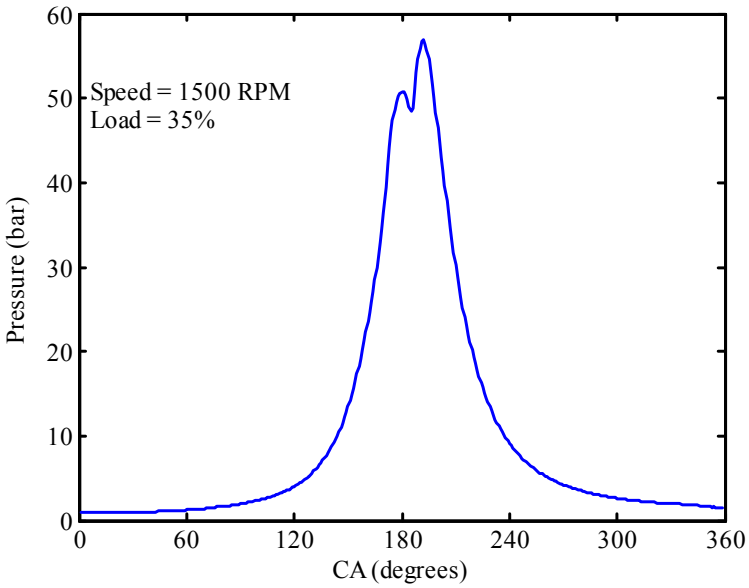

Figure 19. Averaged Smoothed Cylinder Pressure versus °CA (1500 RPM and 35% load)

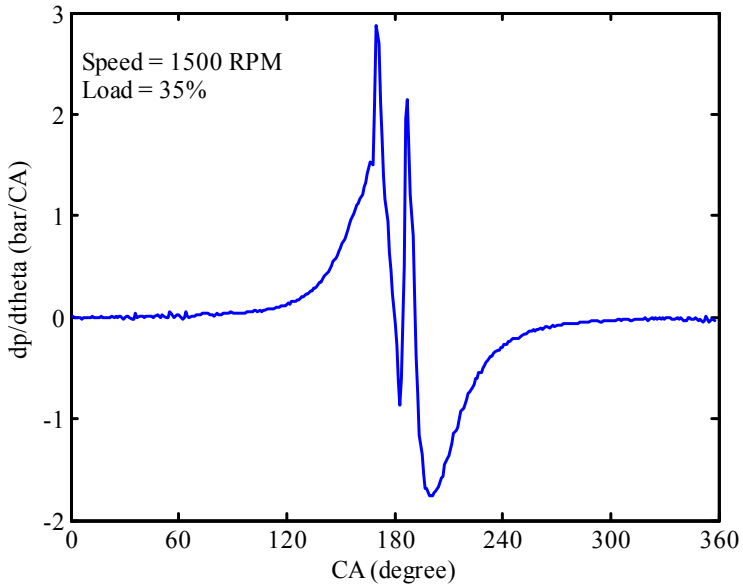

Figure 20. Rate of Change of Pressure versus °CA (1500 RPM and 35% load)

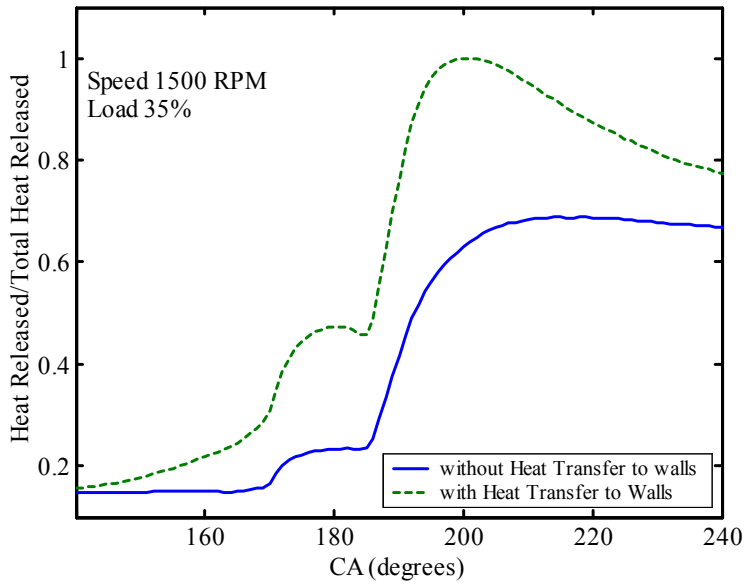

Figure 21. Normalized Heat Released versus °CA (1500 RPM and 35% load)

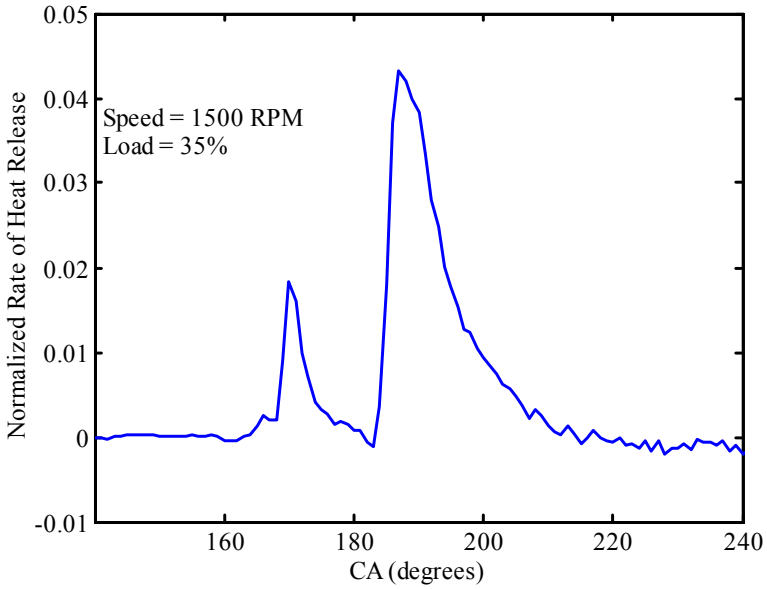

Figure 22. Normalized Rate of Heat Release versus °CA (1500 RPM and 35% load)

Cylinder Pressure Data and Analysis: 1500 RPM and 45% load

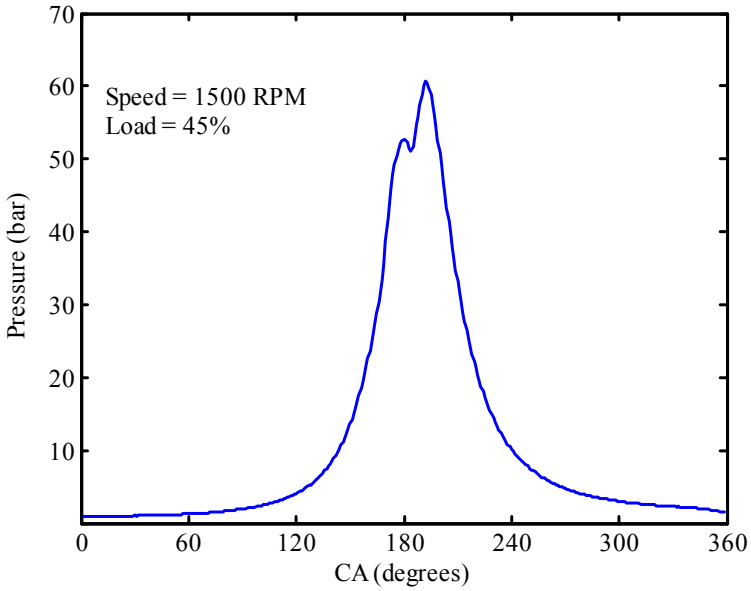

Figure 23. Averaged Smoothed Cylinder Pressure versus °CA (1500 RPM and 45% load)

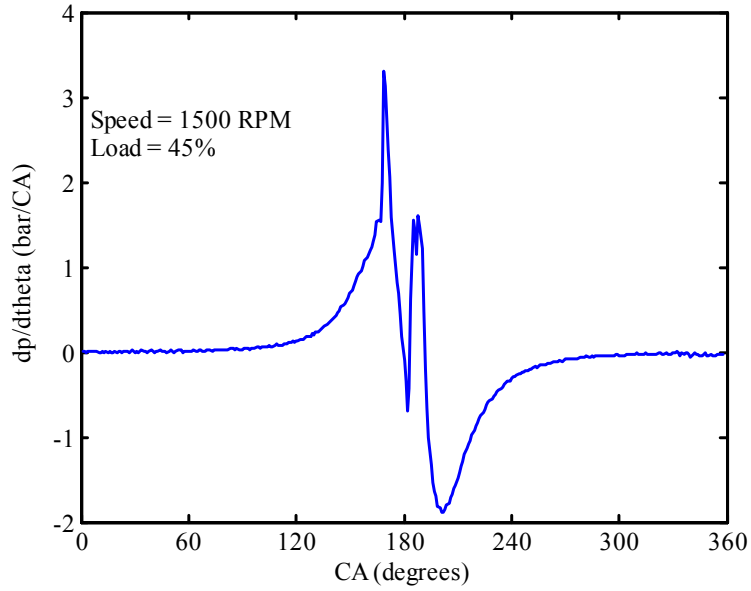

Figure 24. Rate of Change of Pressure versus °CA (1500 RPM and 45% load)

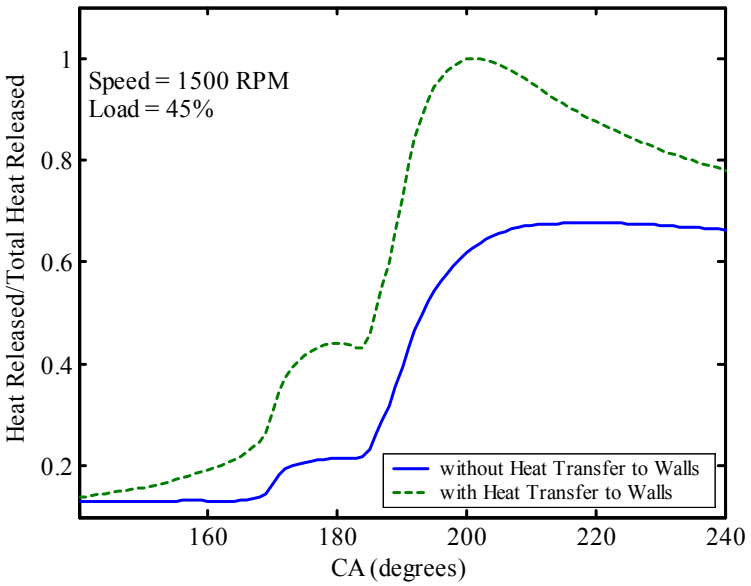

Figure 25. Normalized Heat Released versus °CA (1500 RPM and 45% load)

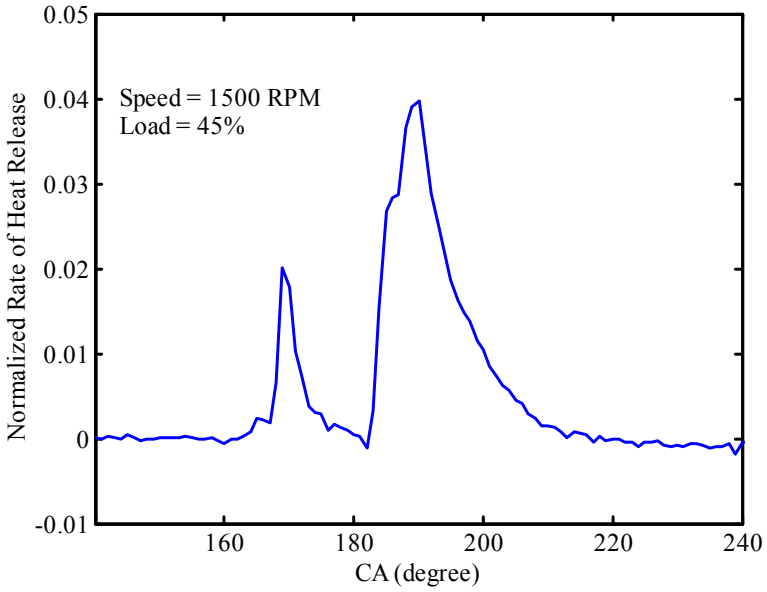

Figure 26. Normalized Rate of Heat Release versus °CA (1500 RPM and 45% load)

Cylinder Pressure Data and Analysis: 1500 RPM & 55% load

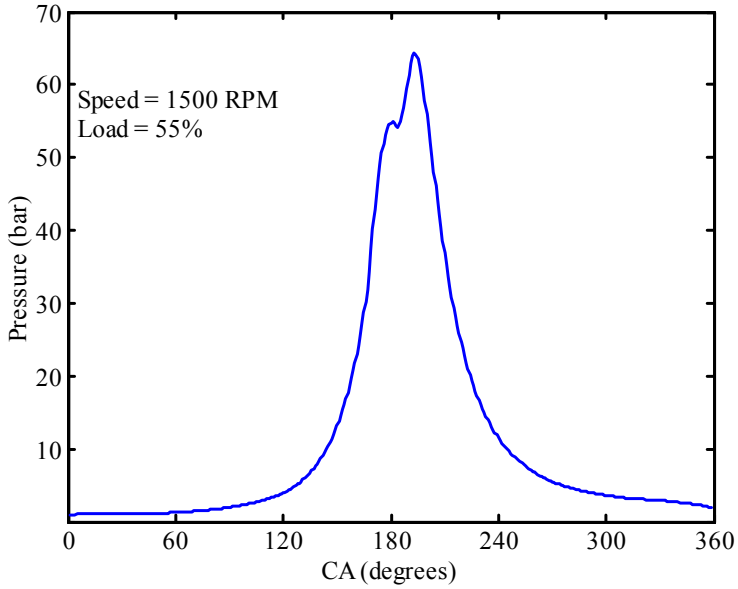

Figure 27. Averaged Smoothed Cylinder Pressure versus °CA (1500 RPM and 55% load)

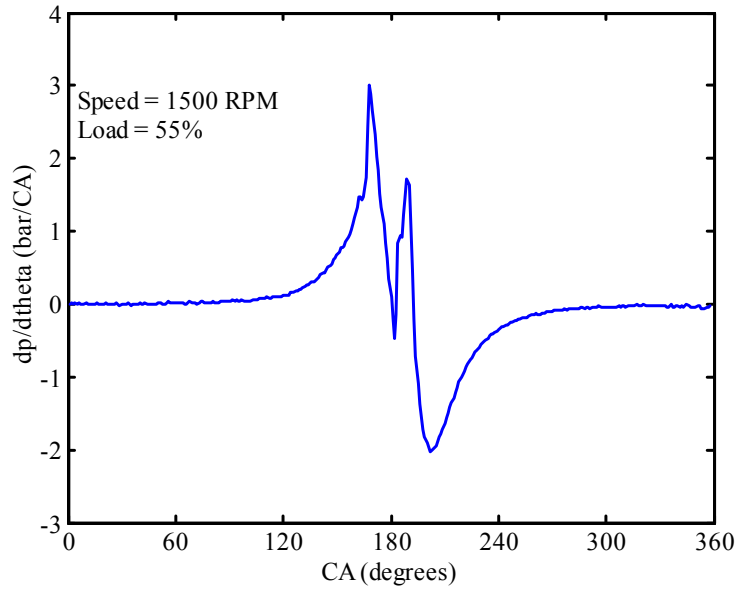

Figure 28. Rate of Change of Pressure versus °CA (1500 RPM and 55% load)

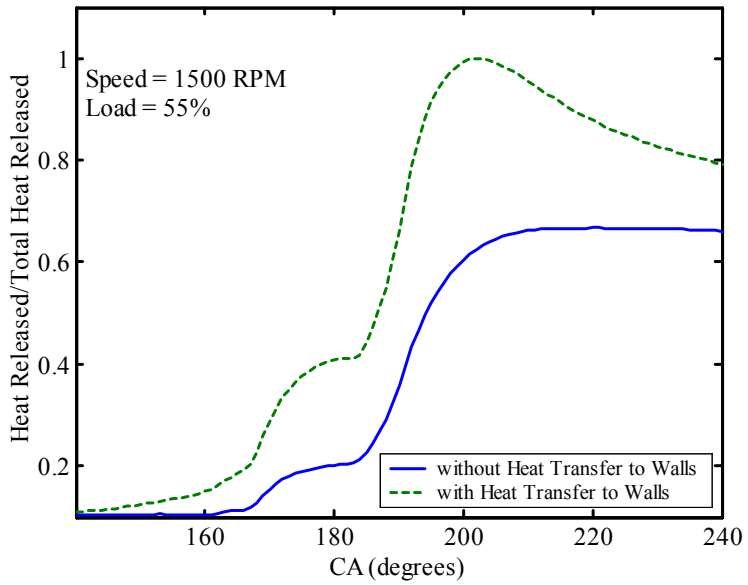

Figure 29. Normalized Heat Released versus °CA (1500 RPM and 55% load)

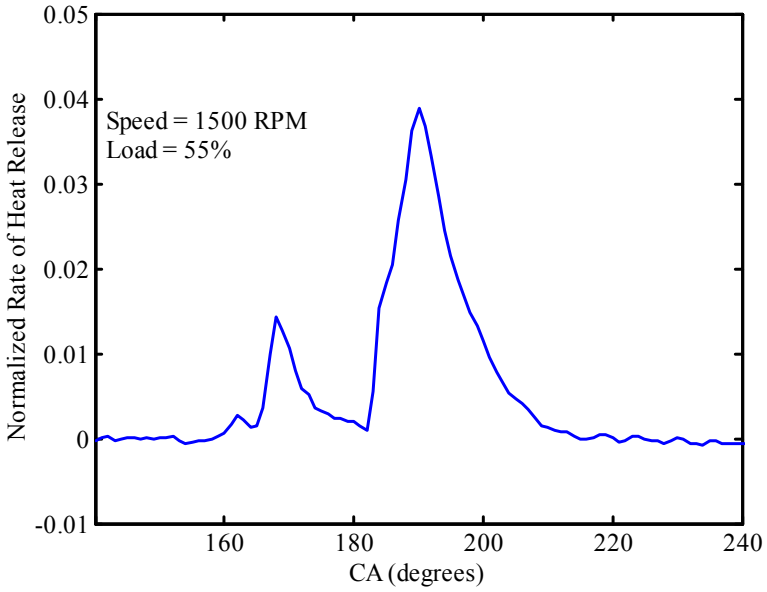

Figure 30. Normalized Rate of Heat Release versus °CA (1500 RPM and 55% load)

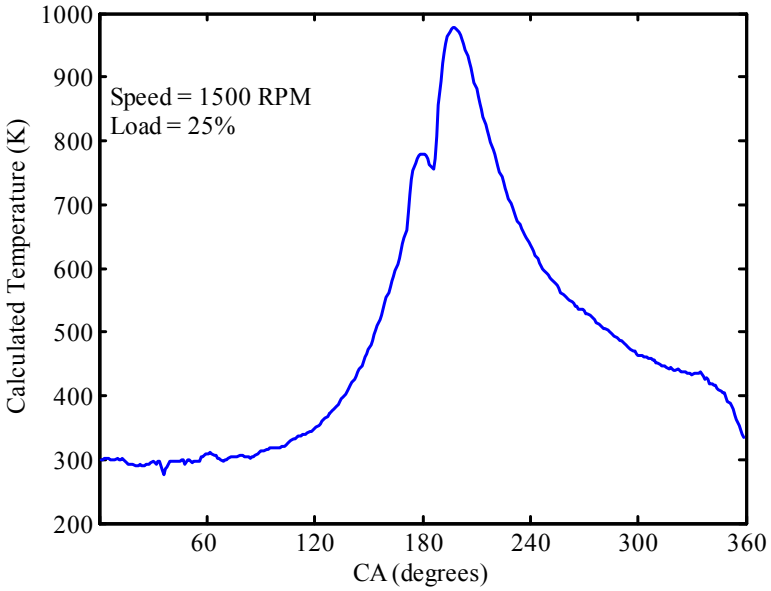

Figure 31. Calculated temperature (K) versus °CA (1500 RPM and 25% load)

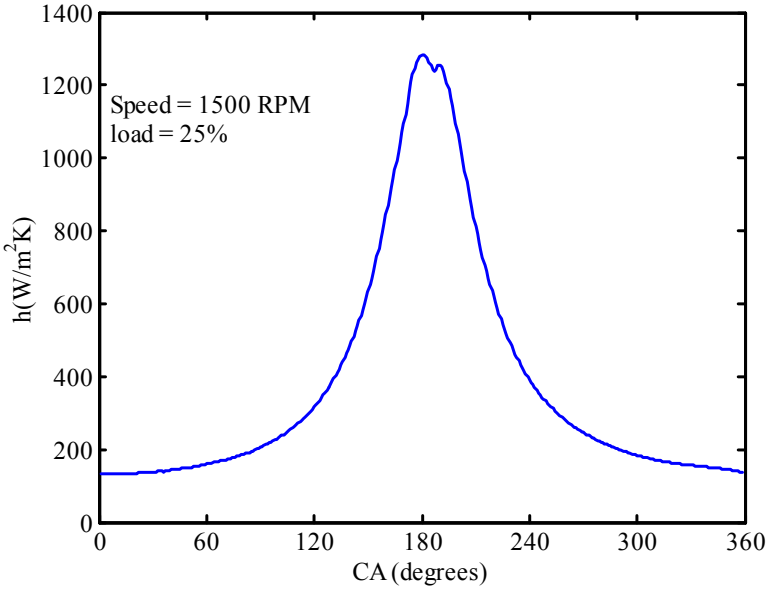

Figure 32. Heat Release Coefficient (h) versus °CA (1500 RPM and 25% Load)

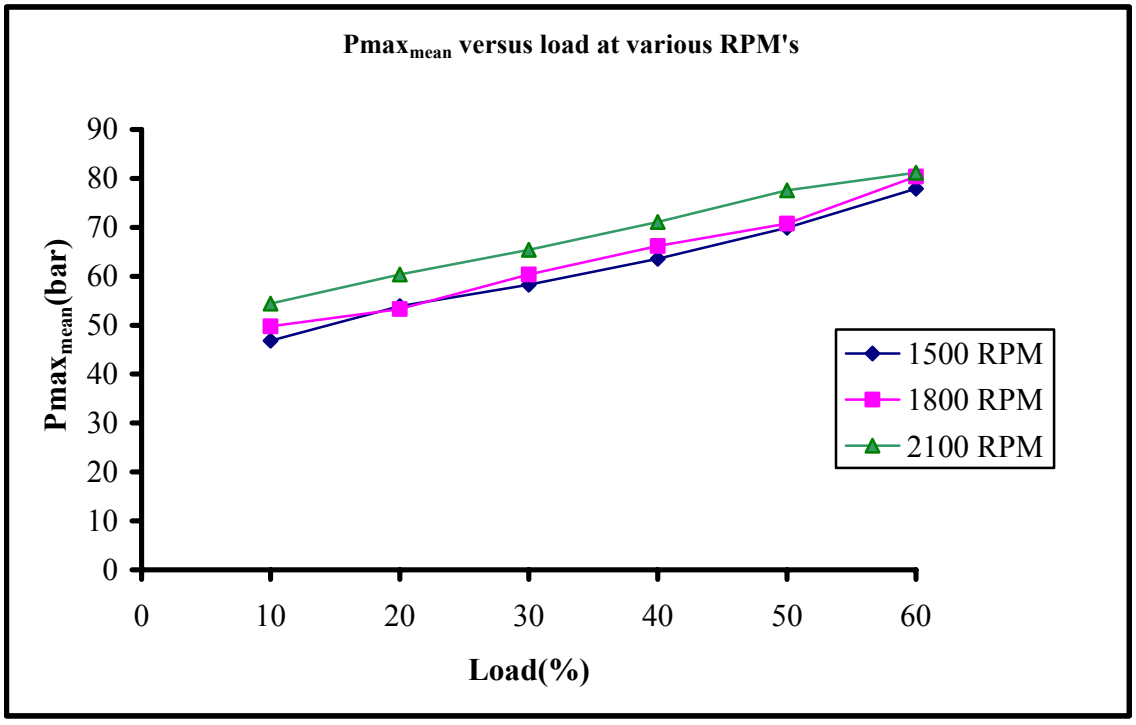

Figure 33. Pmax$_{mean}$ versus load at various speeds

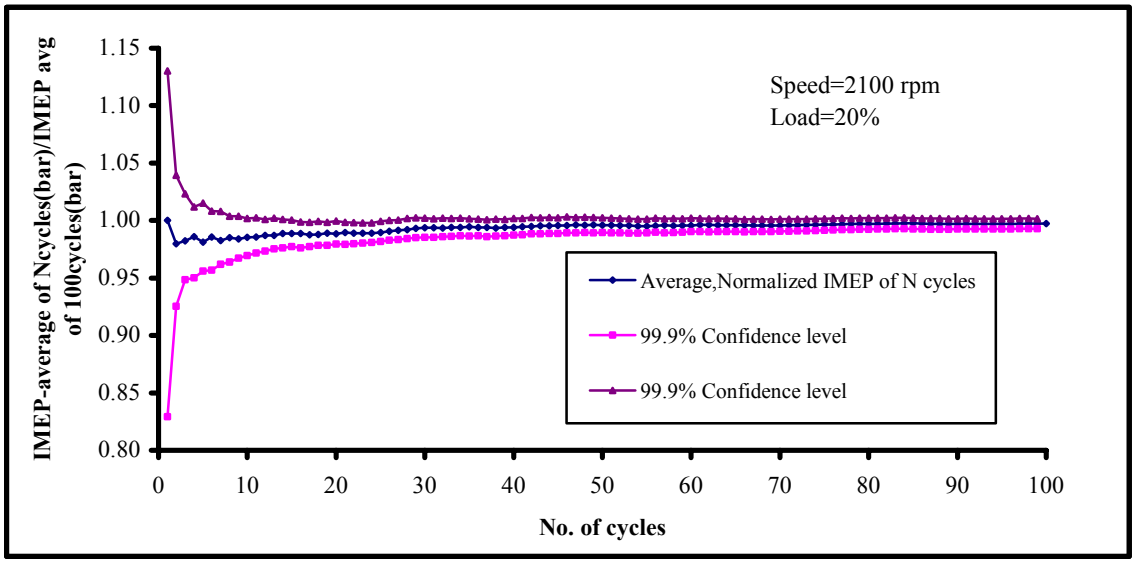

Figure 34. Average, Normalized IMEP versus Number of Cycle

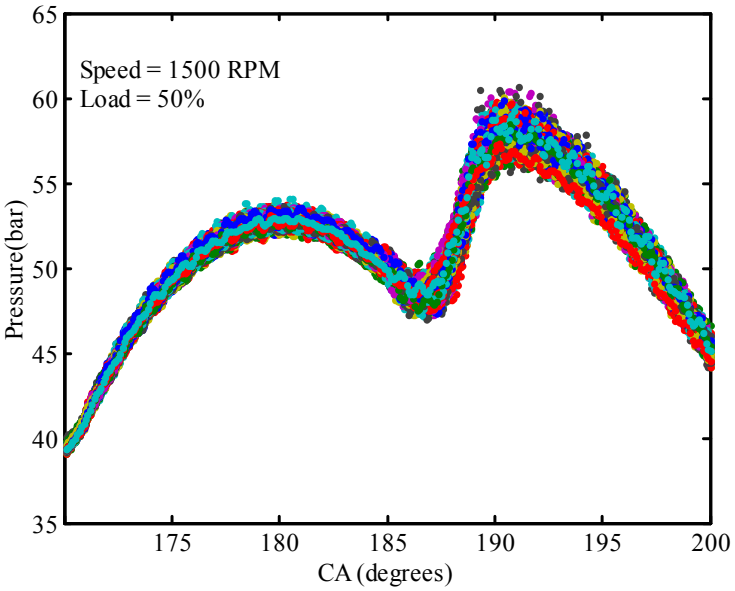

Figure 35. Cylinder Pressure versus °CA for 200 cycles (1500 RPM and 50% Load)

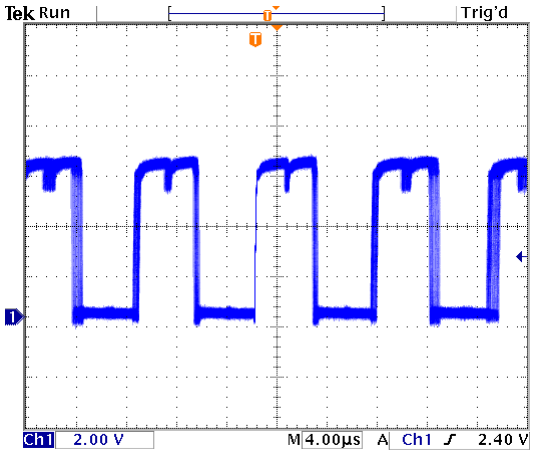

Figure 36. 0.1°CA Signal from the Encoder (from Oscilloscope)

Figure 35 shows the cylinder pressure data acquired for 200 consecutive cycles and Figure 36 shows the 0.1°CA encoder signal as seen in the oscilloscope.

Instantaneous Engine Speed: As mentioned earlier the external clock of the WaveBook/516 was used for data recording. The Wavebook has a 32 bit internal counter that calculates and reports the external clock's period. This permits the instantaneous speed of the engine to be calculated (Fig 37). The counter channel was configured in *"Channel Configuration Spreadsheet"* by turning the CtrLo in on position

The instantaneous engine speed can be used as a diagnostic tool. One method of detecting engine misfire is to examine variations in the instantaneous engine speed. Real-time identification of the misfiring cylinder is especially important in the case of gasoline engines because misfiring may adversely affect the catalytic converter. Real-time misfire detection can be done in the following way: When an engine is operating correctly, the instantaneous speed has a typical shape and regularity. This is measured and recorded. However, when the engine is misfiring the frequency distribution changes and this allows misfire detection.

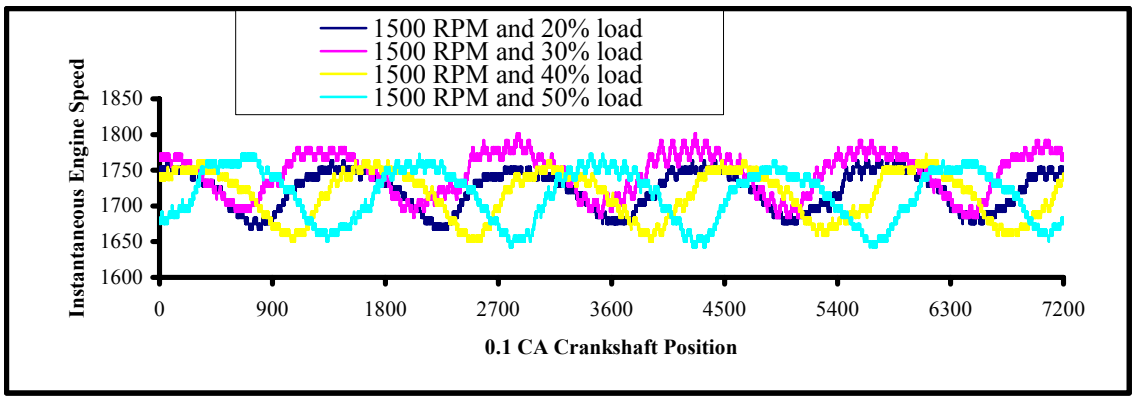

Figure 37. Instantaneous engine speed versus °CA

CHAPTER IV
MODELING AND ANALYSIS

4.1 Heat Release Analysis-Combustion Process Modeling

A variety of simulation models is used to predict the combustion process in diesel engines. These models range from simple empirical zero-dimensional models to highly sophisticated three-dimensional models. Empirical zero-dimensional models are used when the prediction of output performance is the main criteria. Three-dimensional models are used to provide results that are strongly affected by local conditions such as soot or NOx; in other words, when the prediction of emissions is the target.

For empirical zero-dimensional modeling, the heat release approach is commonly used. In this, the thermal effects of combustion, rather than the process itself are modeled. Expressions are developed which correlate the gross heat release rate to the cylinder pressure trace using first law of thermodynamics. The generated heat release data can be presented using mathematical tools such as Weibe functions. These models consist of coefficients whose values need to be determined experimentally. The models can be verified by comparing the predicted cylinder pressure with the experimentally obtained cylinder pressure. The heat-release model should include:

a) An empirical or analytical description of ignition delay,

b) An expression for the heat released during the pre-mixed phase,

c) An expression for the heat released during the diffusion phase

4.1.1 Ignition Delay Modeling

The ignition delay is defined as the time between the start of injection and the apparent start of combustion. It would be justified to distinguish the ignition delay of pilot injection from the ignition delay of the main injection when split injection is implemented [19]. The ignition delay is modeled with an Arrhenius type of correlation. The three important variables to be taken into account for ignition delay modeling are mean temperature, mean pressure and load. Engine load is given in terms of the percentage of maximum torque output.

$$\tau = a\phi^{b}\left(Pm\right)^{c}\exp(d/Tm) \qquad (4.1)$$

where, τ = Ignition delay in Crank Angles.

ϕ = Load (in percentage)

P_m = Mean Cylinder Pressure

T_m = Mean Combustion Chamber Temperature.

a, b, c and d are the constants to be determined

For the ignition delay of the main combustion, it may be noted that fuel injection is not terminated during the ignition delay period and affects the ignition process.

4.1.2 Premixed and Diffusion Burning Modeling

In a common-rail diesel engine, the pilot injection burning was approximated as premixed combustion and the main injection burning was approximated as diffusion burning. The total heat released is the sum of heat released during the premixed and the diffusion phase. Weibe functions were used to describe the heat released in both the

premixed and the diffusion phases. Heat Release curves has an essentially universal dimensionless curve [3]. This s-shaped curve is often represented by the Weibe function:

$$Q(\alpha) = Qtotal\left(1 - \exp\left[-a\left(\frac{\theta - \theta_0}{\Delta\theta}\right)^{m=1}\right]\right) \tag{4.2}$$

where,

θ is the crank angle, θ_0 is the start of combustion, $\Delta\theta$ is the total combustion duration and a and m are adjustable parameters which fix the shape of the curve.

4.1.3 Derivation of Pressure versus Crank Angle for Finite Heat Release

The differential first law for this model for a small crank angle change, dθ, is:

$$\partial Q - \partial W = dU \tag{4.3}$$

Using the following definitions, ∂Q=heat release, $\partial W = PdV$ and $dU = mC_v dT$, results in

$$\partial Q - PdV = mC_v dT \tag{4.4}$$

The ideal gas equation is PV = mRT, so

$$mdT = \frac{1}{R}(PdV + VdP) \tag{4.5}$$

and

$$dU = \frac{C_v}{R}(PdV + VdP) \tag{4.6}$$

The first law now becomes

$$\partial Q - PdV = \frac{C_v}{R}(PdV + VdP) \tag{4.7}$$

Further reducing the equation:

$$\frac{\partial Q}{\partial \theta} - \left(1 + \frac{C_v}{R}\right) P \frac{dV}{d\theta} = \frac{C_v}{R} V \frac{dP}{d\theta} \tag{4.8}$$

Using $R = C_p - C_v$ and $\gamma = C_p/C_v$, , the energy equation after rearrangement becomes:

$$\frac{dP}{d\theta} = \frac{\gamma - 1}{V} \frac{\partial Q}{\partial \theta} - \frac{P}{V} \frac{dV}{d\theta} \tag{4.9}$$

If we know the pressure, P, volume, V, $\frac{dV}{d\theta}$, the heat released gradient, $\frac{\partial Q}{\partial \theta}$, we can compute the change in pressure, $\frac{dP}{d\theta}$. Thus explicitly solving the equation for pressure as a function of crank angle.

First, the volume, V and $\frac{dV}{d\theta}$ have to be defined. From the slider-crank model, we have a definition for cylinder volume, V. Both terms are only dependent on engine geometry.

$$V = \frac{V_d}{r - 1} + \frac{V_d}{2}\left[R + 1 - \cos\theta - \sqrt{R^2 - \sin^2\theta}\right)\Big] \tag{4.10}$$

where, V_d is the displacement volume, r is the compression ratio, θ is the instantaneous crankangle position (θ=0 is at TDC) and R is the ratio of the connecting rod length to the crank radius.

So taking the derivative with respect to the crank angle, θ, results in:

$$\frac{dV}{d\theta} = \frac{V_d}{2} \sin\theta \left[1 + \frac{\cos\theta}{\sqrt{R^2 - \sin^2\theta}}\right] \tag{4.11}$$

Equation (4.8) was solved using a MATLAB program provided by Dr. Al Kornhauser.

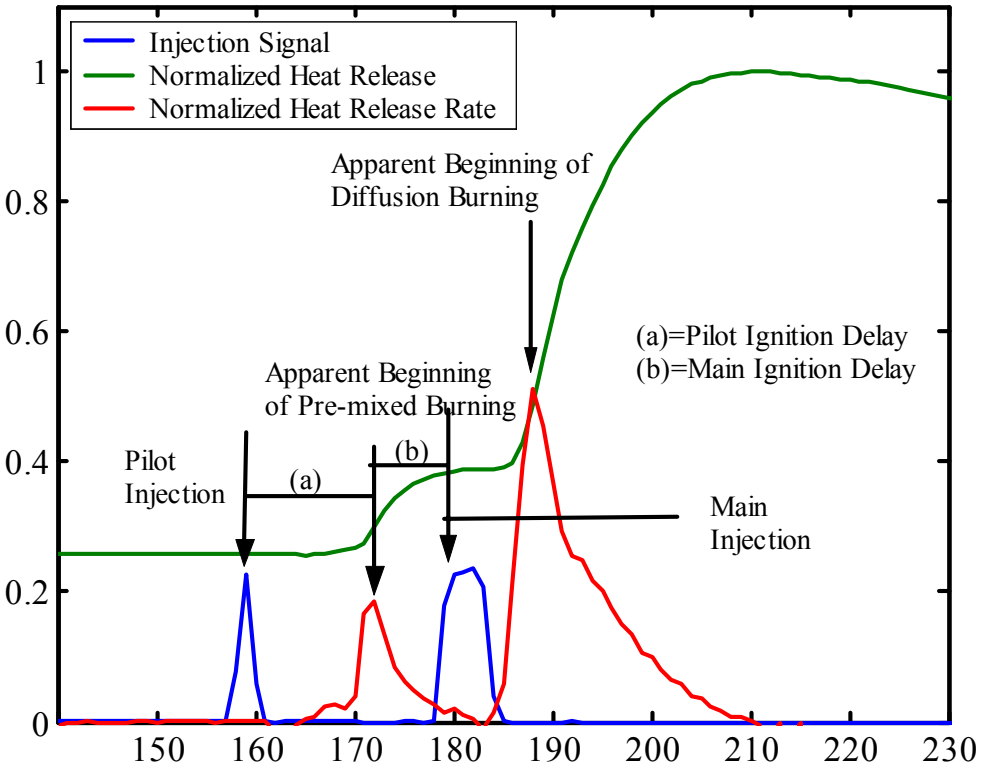

Figure 38. Various Stages of Combustion in Common-Rail Engines

Figure 38 shows the various stages of combustion in common rail diesel engine. This figure was plotted for each of the engine operating condition analyzed to determine the values of the pilot and main injection ignition delay.

Determination of the pilot injection and main injection ignition delay: The fuel injection signal has two distinct parts: one corresponding to pilot injection and the second corresponding to the main injection. The positions (in crank angles) where these two parts attain their maximum for the first time is noted as the beginning of the pilot and the main injection. Similarly, the normalized heat release rate diagram has two parts: one

corresponding to the pilot burning and the second corresponding to the main burning. The position (in crank angles) for the peak of the first part is taken as the apparent pilot injection combustion starting point. The difference (in crank angles) between the pilot injection beginning point and the pilot injection combustion beginning point is the pilot injection ignition delay in crank angles. The same procedure was repeated to find the main injection ignition delay in crank angle.

In the normalized heat release plot, it can be seen that the pilot burning curve shows a sudden rise and after being flat for some crank angles begins to go down. The point at which it begins to go down is noted as the end-point of pilot combustion. The same procedure is adopted to find the end-point of main combustion

CHAPTER V
RESULTS and CONCLUSION

Conclusion

The following are the conclusions based on the this research:

- A combustion data acquisition system was developed and successfully tested, using generic hardware components available. This setup can record cylinder pressure data every 0.1°CA at a variable sampling speed. The setup also has provision for recording the fuel injection signal for one injector.
- MATLAB programs were developed as part of the research to conduct heat release analysis.
- Based on the heat release analysis a two Weibe function, heat release model has been proposed. Preliminary analysis has shown that the predicted cylinder pressure trace is close to the actual cylinder pressure trace.

The ignition delays for engine conditions of 1500 RPM and between 25% and 55% load were evaluated using the fuel injection, heat release/CA and rate of heat release versus CA data for both the pilot and the main injection as listed in Table 3 and Table 5. Subsequently, least-square method was used to evaluate the constants (Table 4 and 6). The data has been presented graphically in Figures 39 and 40. As described earlier, the Weibe function was used to model pre-mixed and diffusion burning. The comparison of actual versus predicted heat release is shown for 1500 RPM at different loads in Figures 41 to 54. Table 7 gives the calculated duration of main and pilot burning.

Table 3. Pilot Injection Ignition Delay for different loads

Load (%)	Calculated Pilot Injection Ignition Delay (CA)	*Pm* (Bars)	*Tm* (K)	Predicted (CA)
25	13	19.95	529.89	11
30	13	19.88	527.86	11
35	12	19.98	530.52	11
40	12	19.83	526.51	11
45	12	19.41	533.69	11
50	14	17.38	495.04	18
55	13	17.8	507.00	15

The parameters a, b, c and d were found to be:

Table 4. Constants for pilot injection ignition delay expression

a	b	c	d
2.4	-0.2	-1.02	2700

Table 5. Main injection Ignition delay for different loads

Load (%)	Calculated Main Injection Ignition Delay (CA)	*Pm* (Bars)	*Tm* (K)	Predicted (CA)
25	6	47.83	776.71	6
30	6	49.41	801.40	5
35	5	50.81	823.97	4
40	5	51.92	842.07	4
45	5	52.66	853.94	4
50	3	53.72	872.29	3.5
55	3	54.75	892.57	3

The parameters a, b, c and d were found to be:

Table 6. Constants for main injection ignition delay expression

a	b	c	d
2.4	-0.2	-1.02	2800

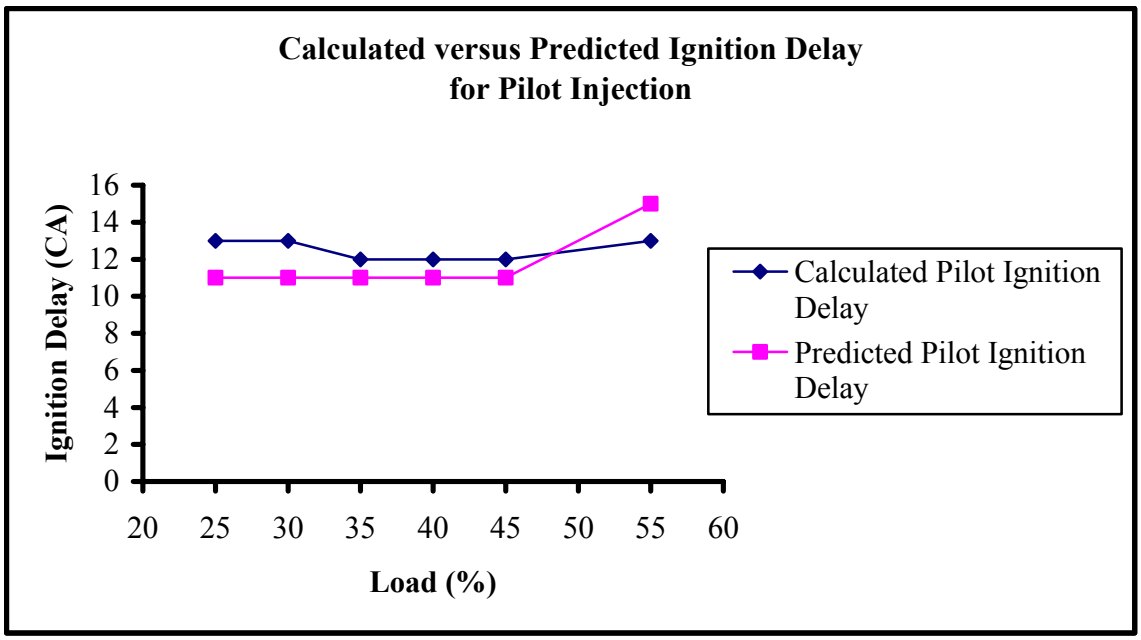

Figure 39. Calculated versus Actual Ignition Delay for Pilot Injection

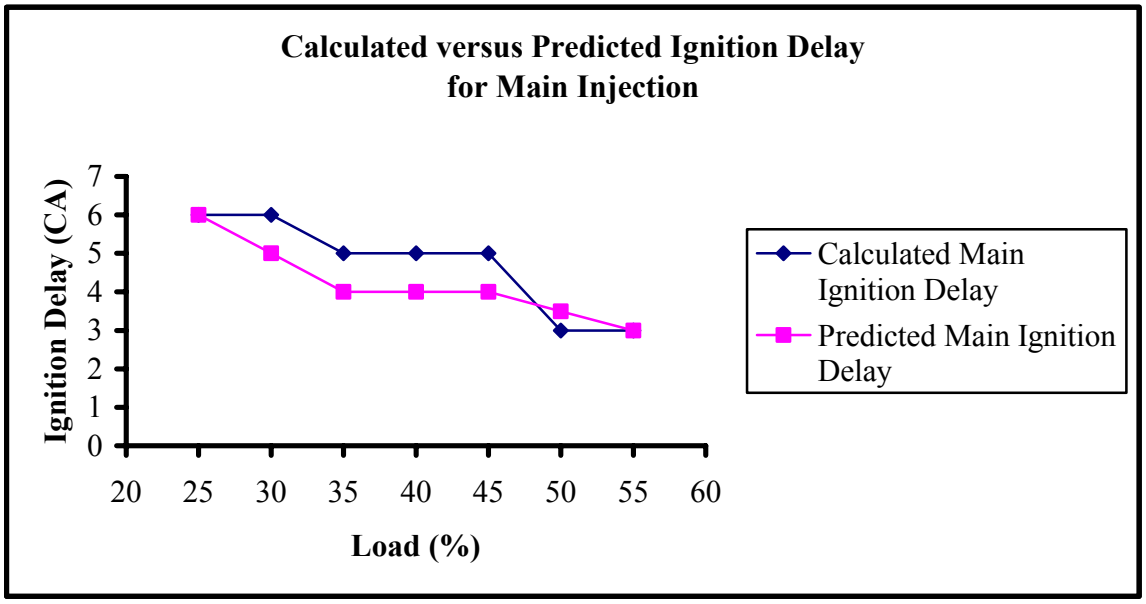

Figure 40. Calculated versus Predicted Ignition Delay for Main Injection

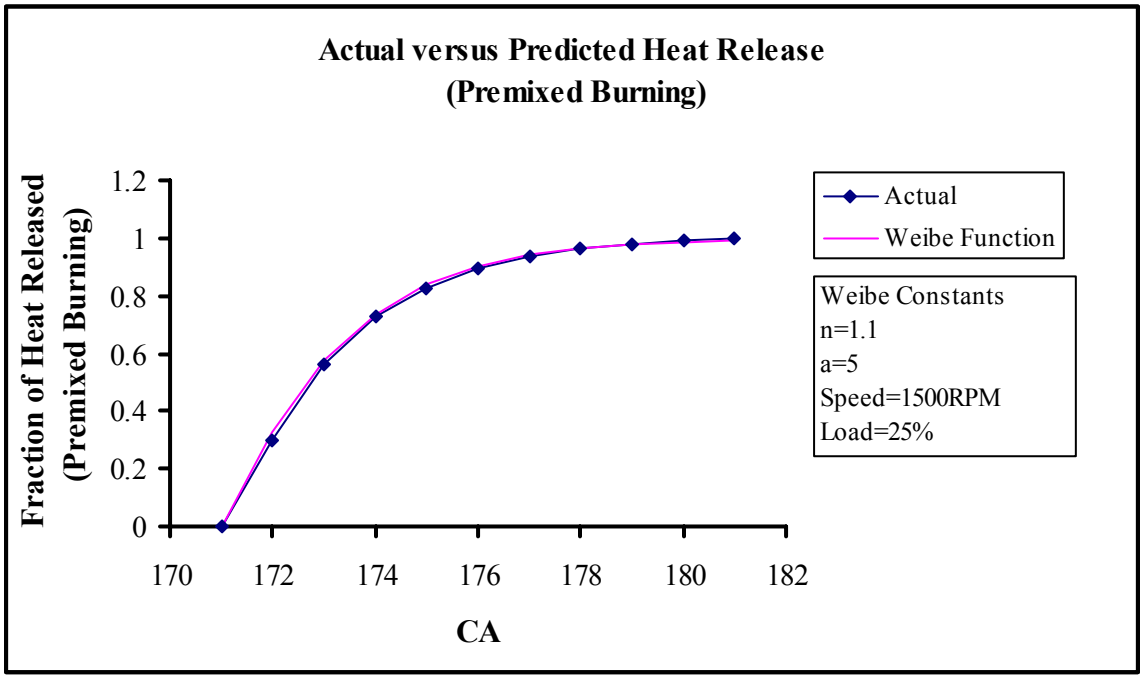

Figure 41. Actual versus Predicted Heat Release (Premixed Burning-1500 RPM and 25% Load)

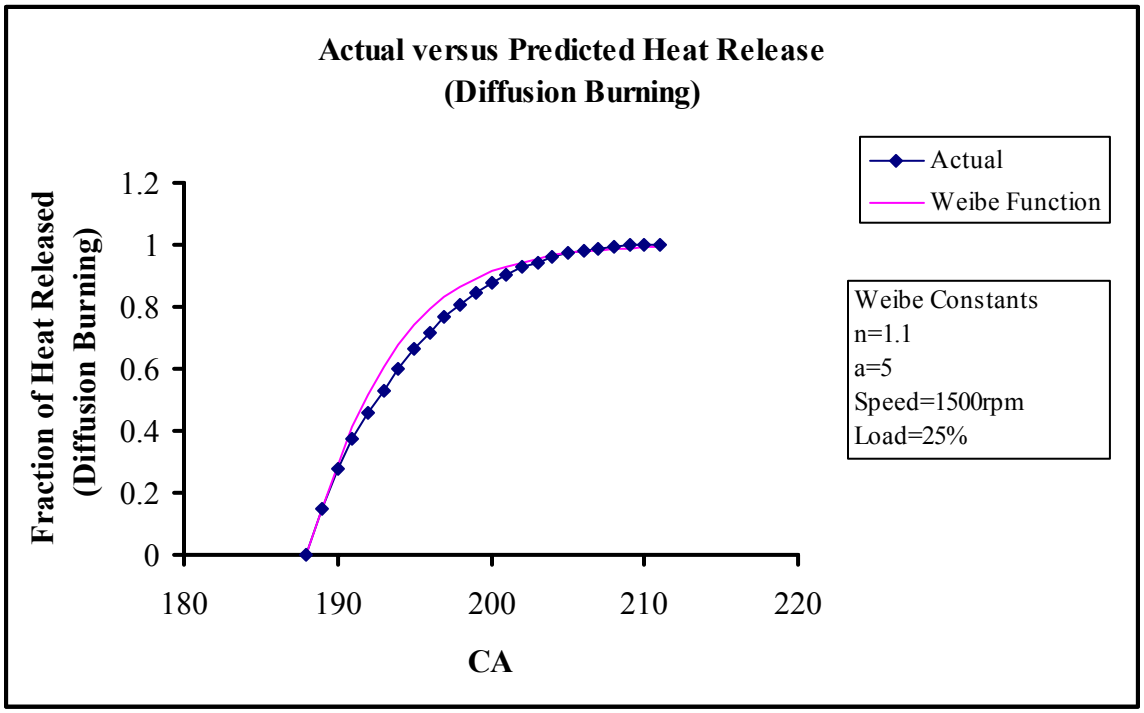

Figure 42. Actual versus Predicted Heat Release (Diffusion Burning-1500 RPM and 25% Load)

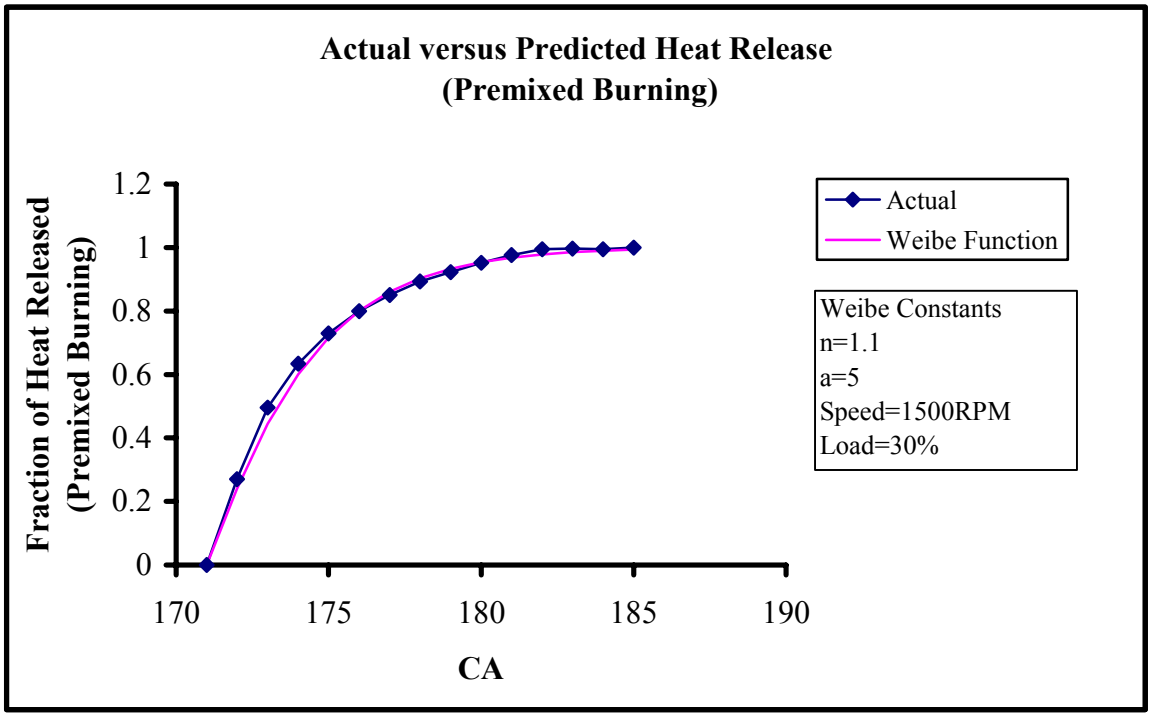

Figure 43. Actual versus Predicted Heat Release (Premixed Burning-1500 RPM and 30% Load)

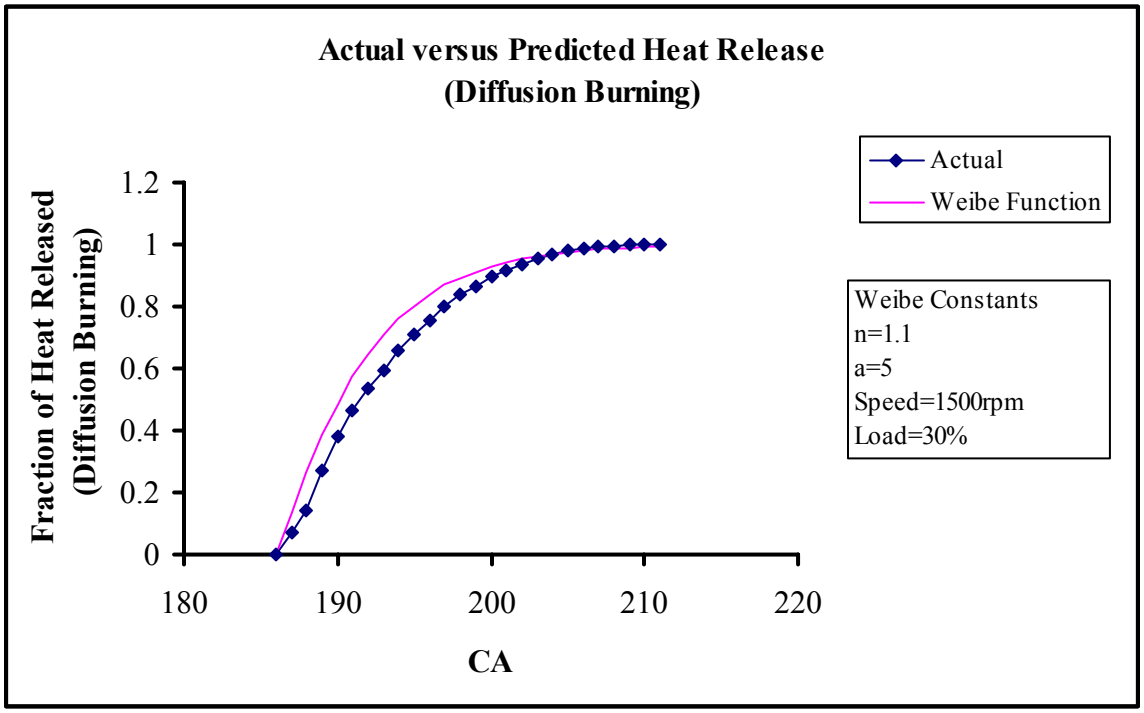

Figure 44. Actual versus Predicted Heat Release (Diffusion Burning-1500 RPM and 30% Load)

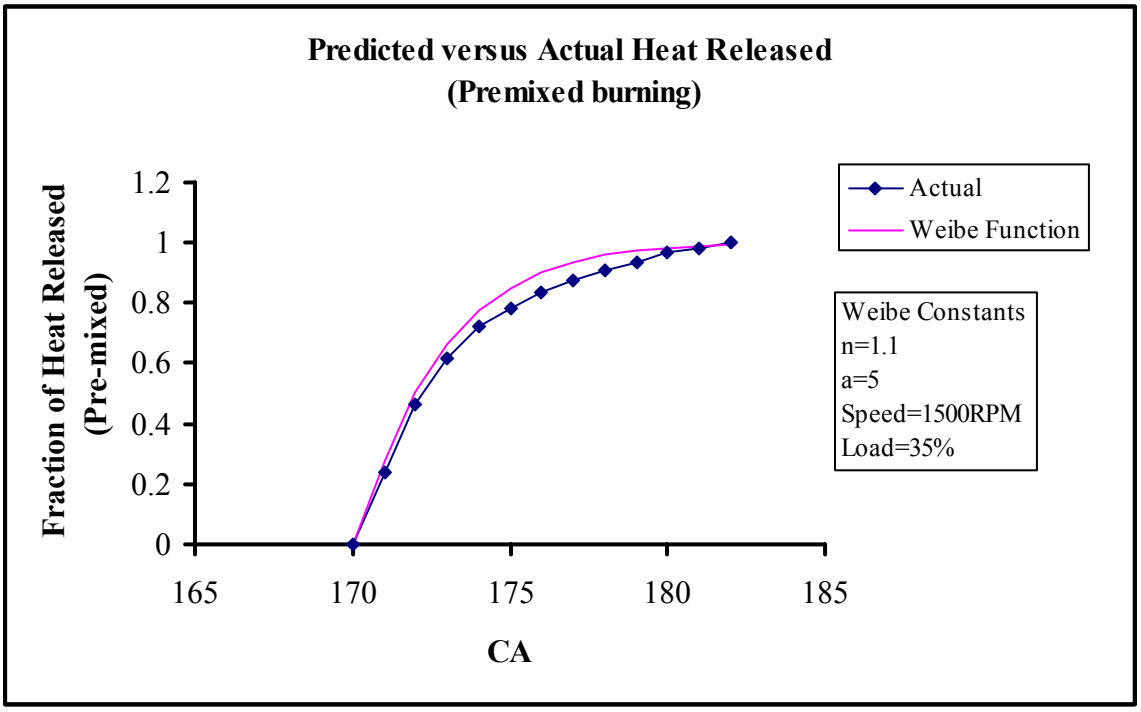

Figure 45. Actual versus Predicted Heat Release (Premixed Burning-1500 RPM and 35% Load)

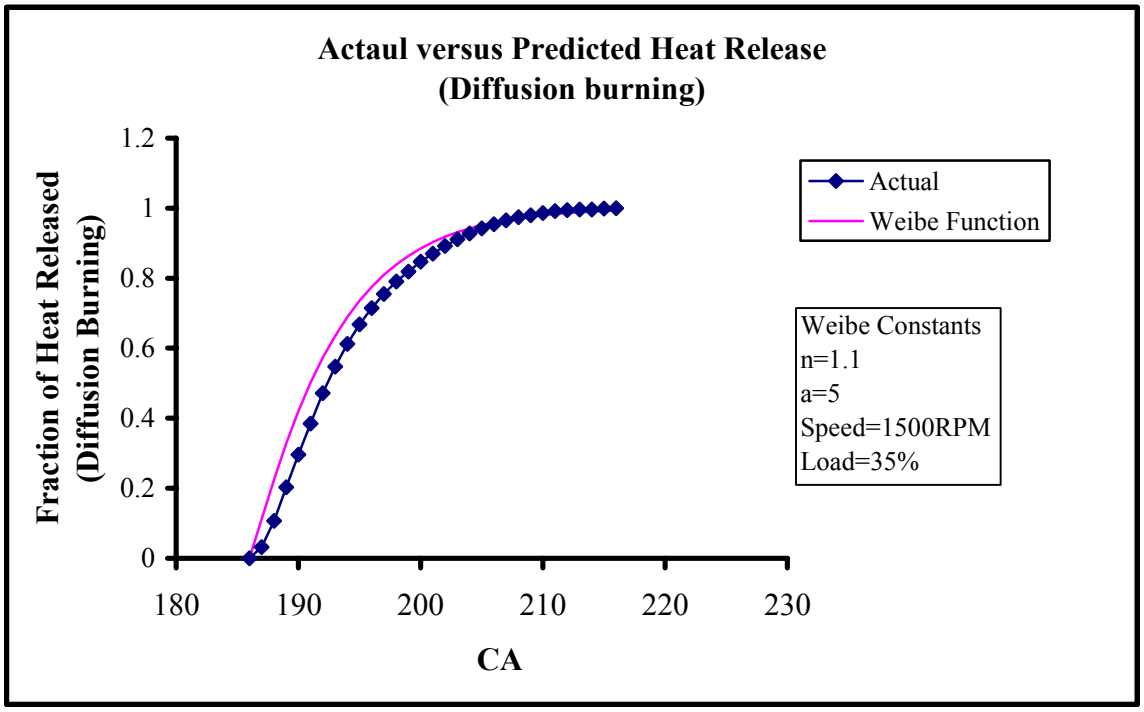

Figure 46. Actual versus Predicted Heat Release (Diffusion Burning-1500 RPM and 35% Load)

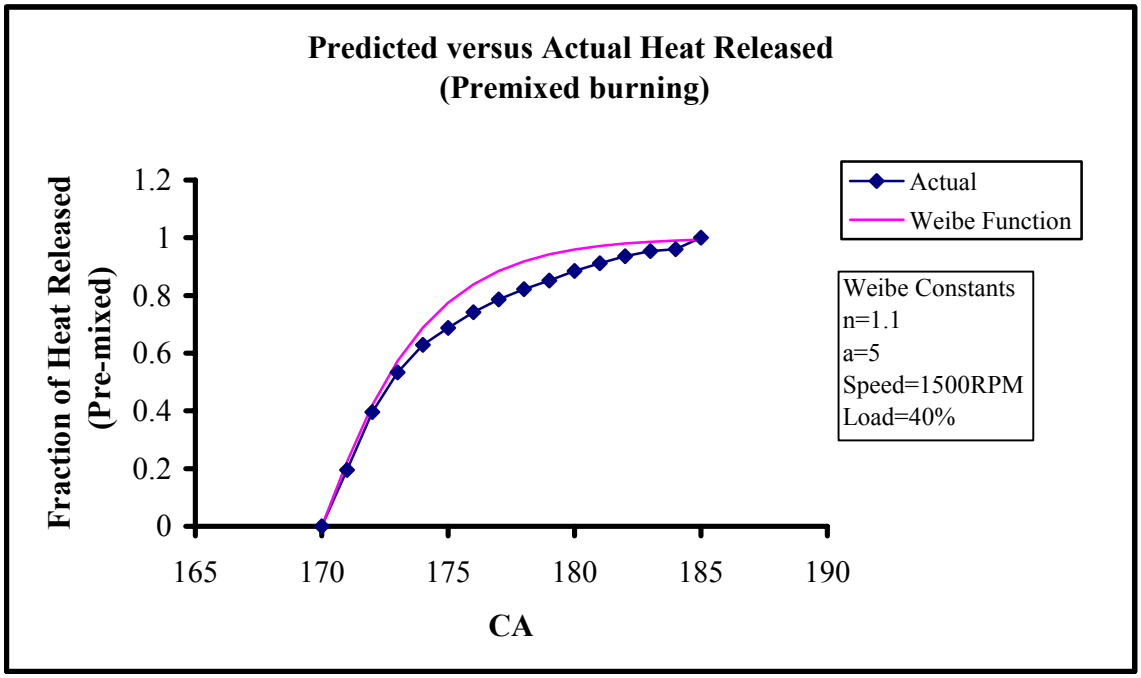

Figure 47. Actual versus Predicted Heat Release (Premixed Burning-1500 RPM and 40% Load)

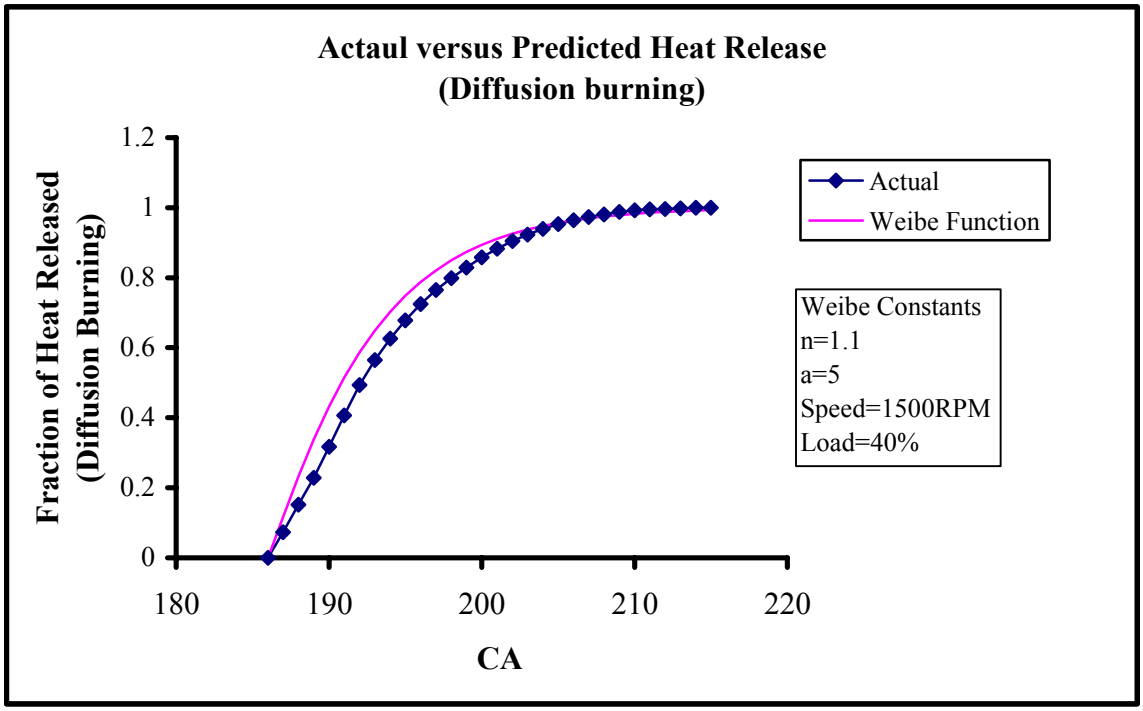

Figure 48. Actual versus Predicted Heat Release (Diffusion Burning-1500 RPM and 40% Load)

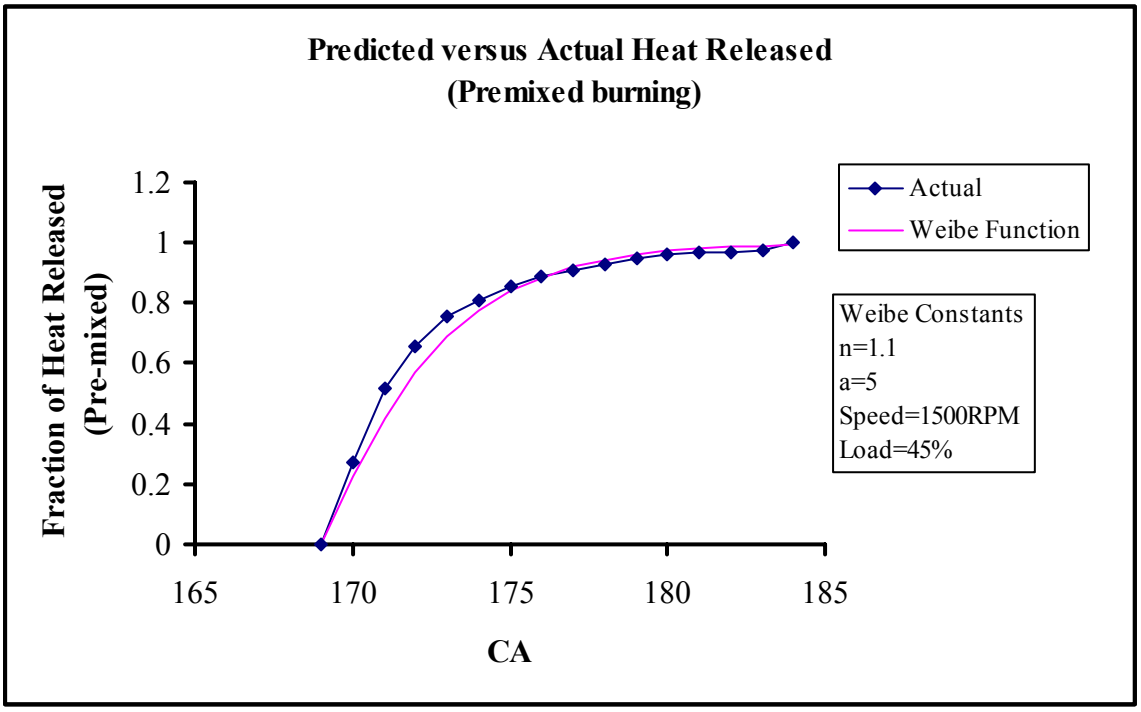

Figure 49. Actual versus Predicted Heat Release (Premixed Burning-1500 RPM and 45% Load)

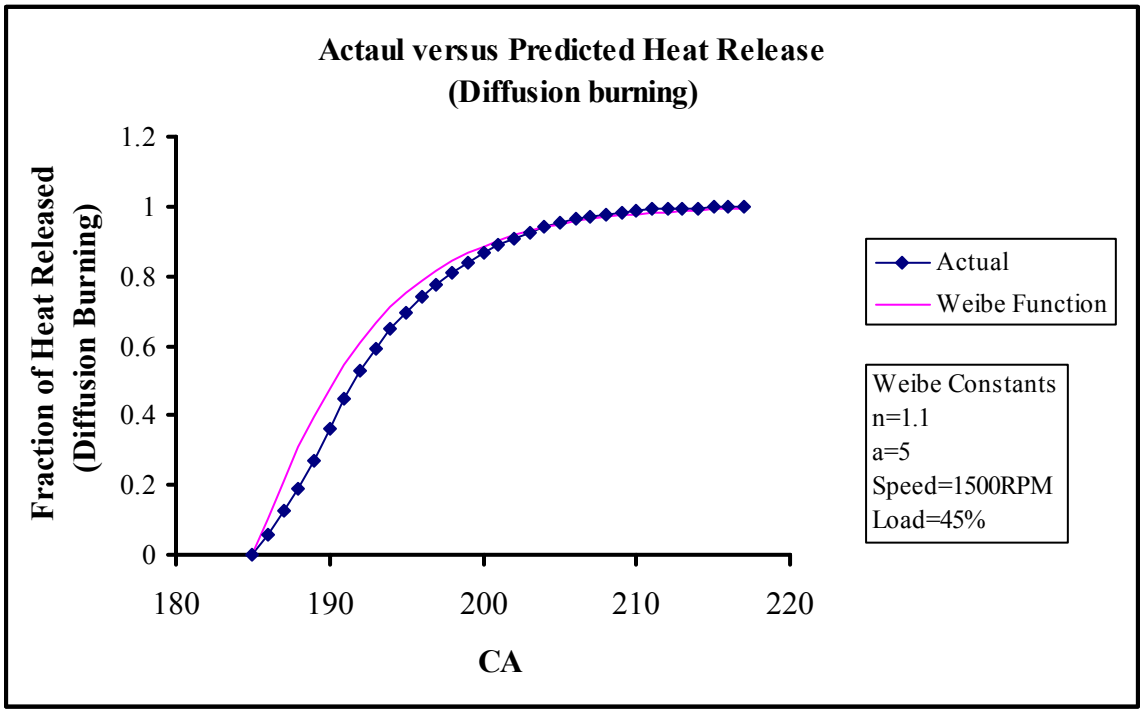

Figure 50. Actual versus Predicted Heat Release (Diffusion Burning-1500 RPM and 45% Load)

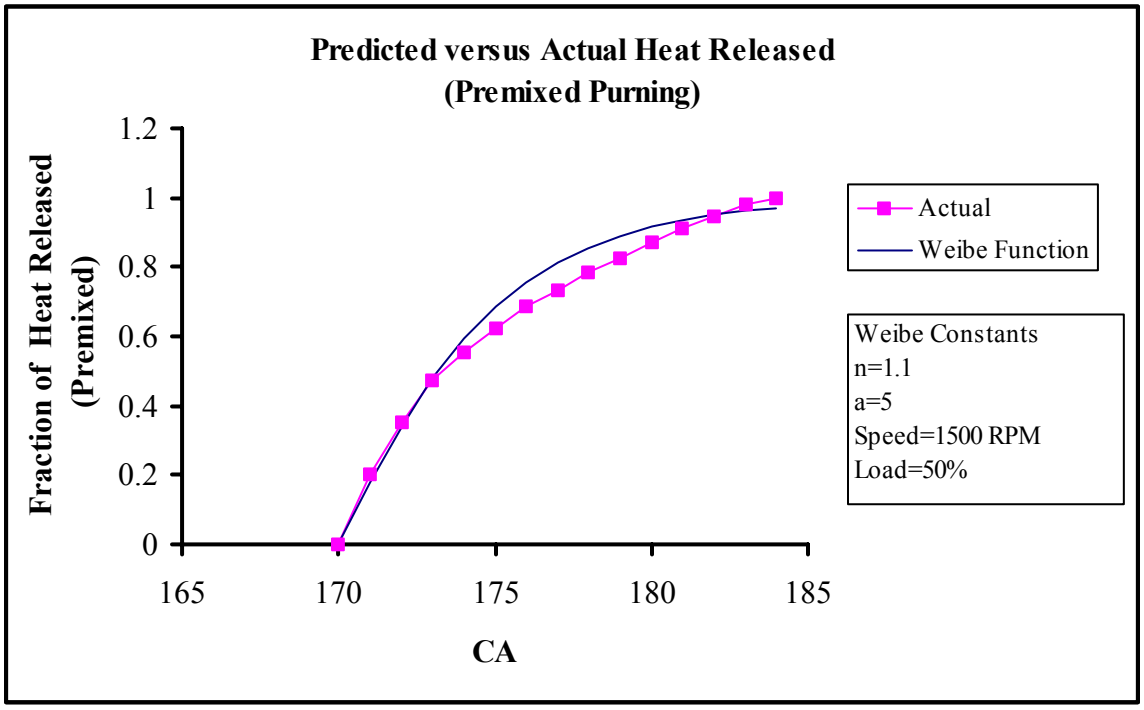

Figure 51. Actual versus Predicted Heat Release (Premixed Burning-1500 RPM and 50% Load)

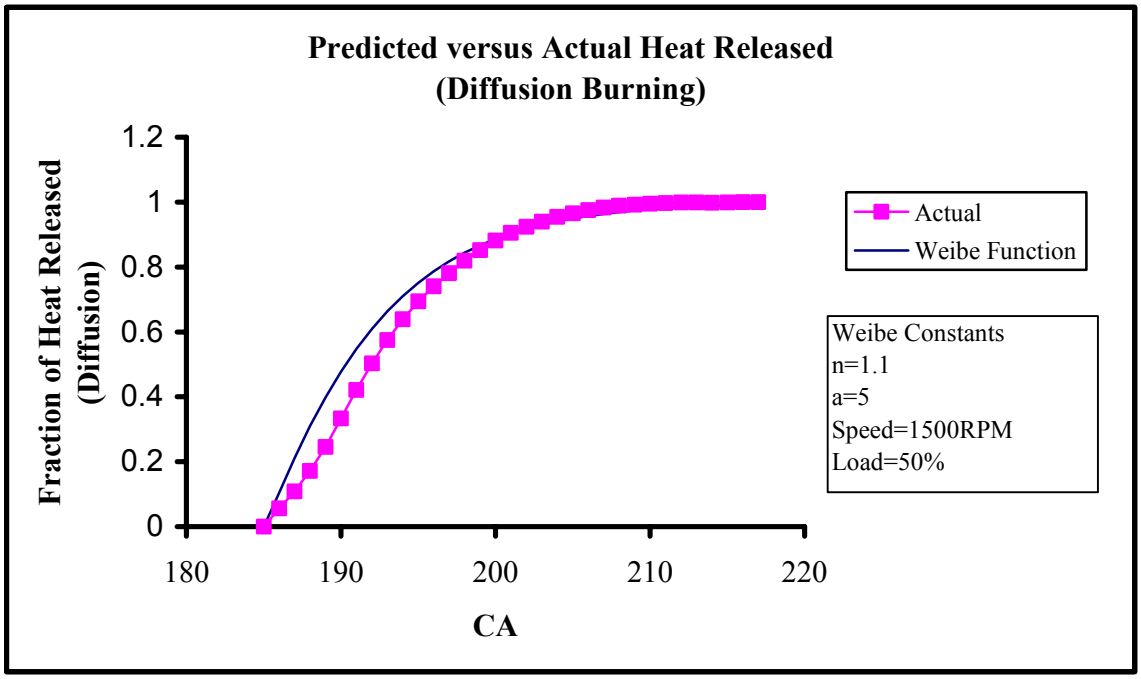

Figure 52. Actual versus Predicted Heat Release (Diffusion Burning-1500 RPM and 50% Load)

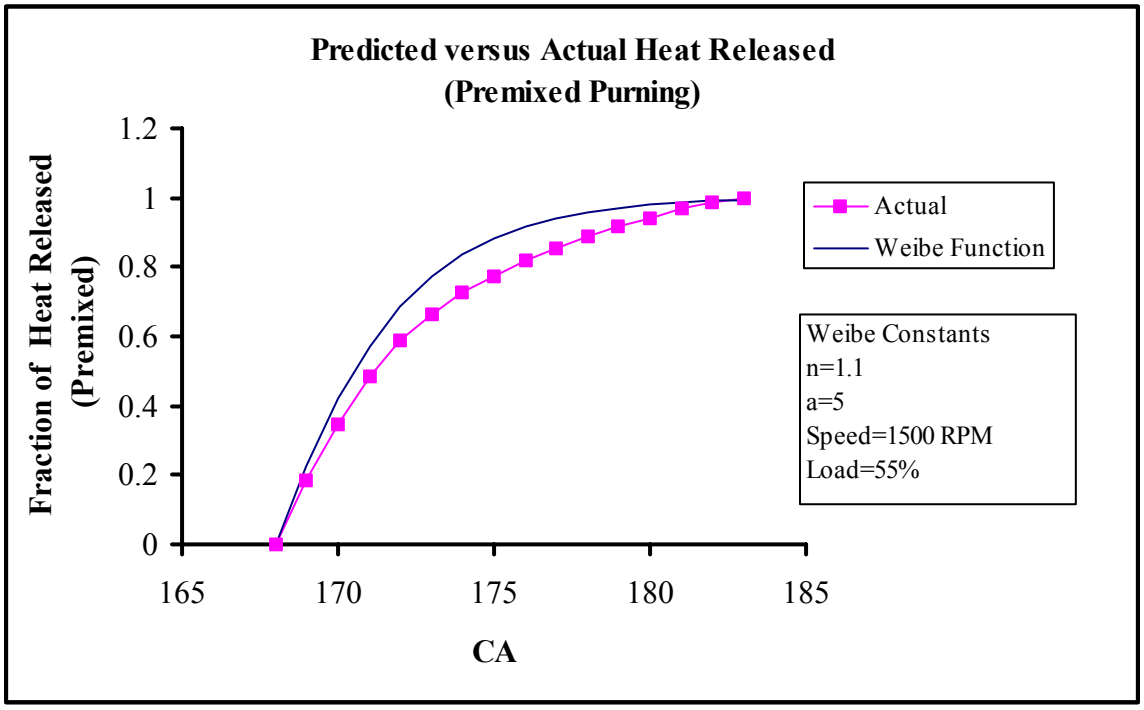

Figure 53. Actual versus Predicted Heat Release (Premixed Burning-1500 RPM and 55% Load)

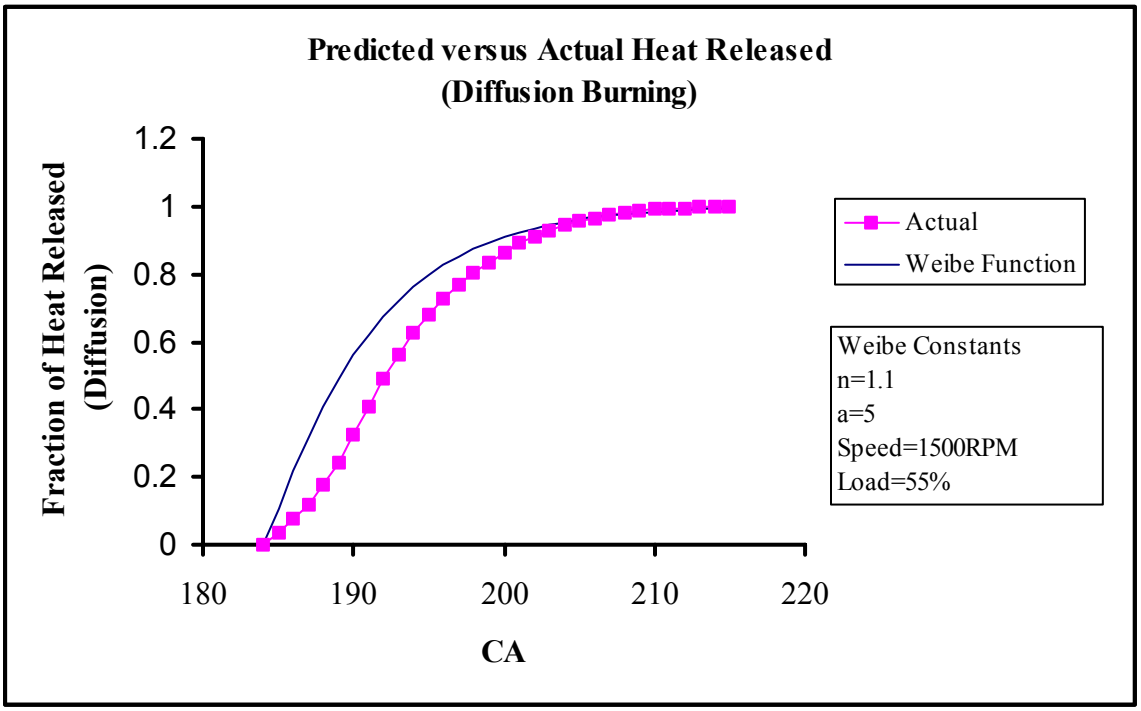

Figure 54. Actual versus Predicted Heat Release (Diffusion Burning-1500 RPM and 55% Load)

Table 7. Duration for Pilot and Main Burning

Load (%)	Duration of pilot Burning	Duration of main Burning
25	10	23
30	14	25
35	12	30
40	15	25
45	15	33
50	14	32
55	15	31

Expression for Heat Release:

Qtotal = Qpilot + Qmain

$$Qpilot = (1.28 * \phi + 34.1392) * (1 - \exp(-5 * (\tau)^{1.3}))) \quad (5.2)$$

$$Qmain = (102.68\, e^{0.00332\varphi}) * (1 - \exp(-5 * (\tau)^{1.3}) \quad (5.3)$$

Where, ϕ = *load* and τ is duration of combustion

Plot for Actual versus Predicted Pressure for various conditions

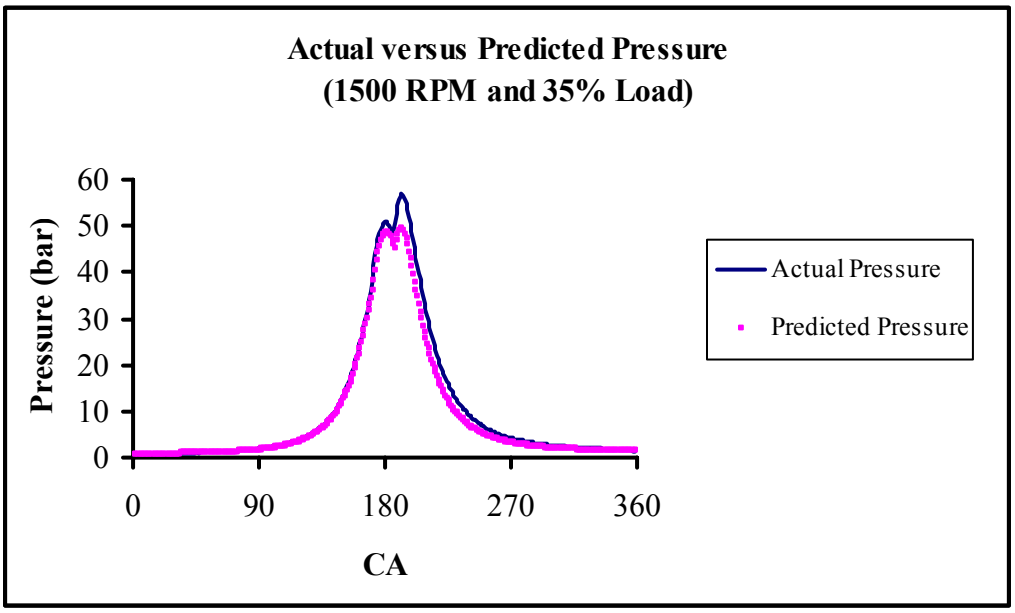

Figure 55. Actual versus Predicted Pressure (1500 RPM and 35% Load)

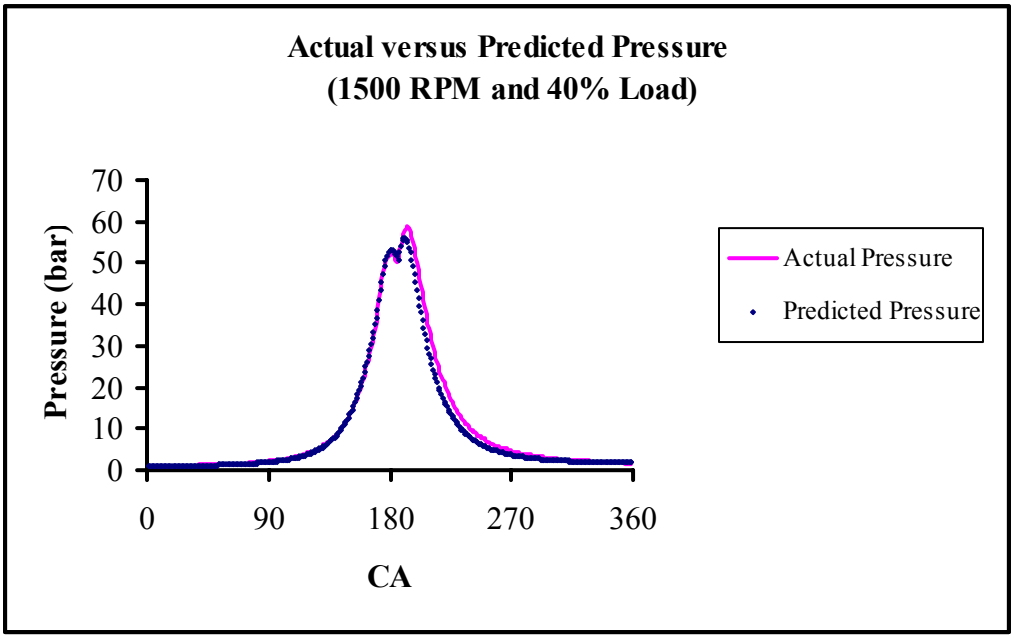

Figure 56. Actual versus Predicted Pressure (1500 RPM and 40% Load)

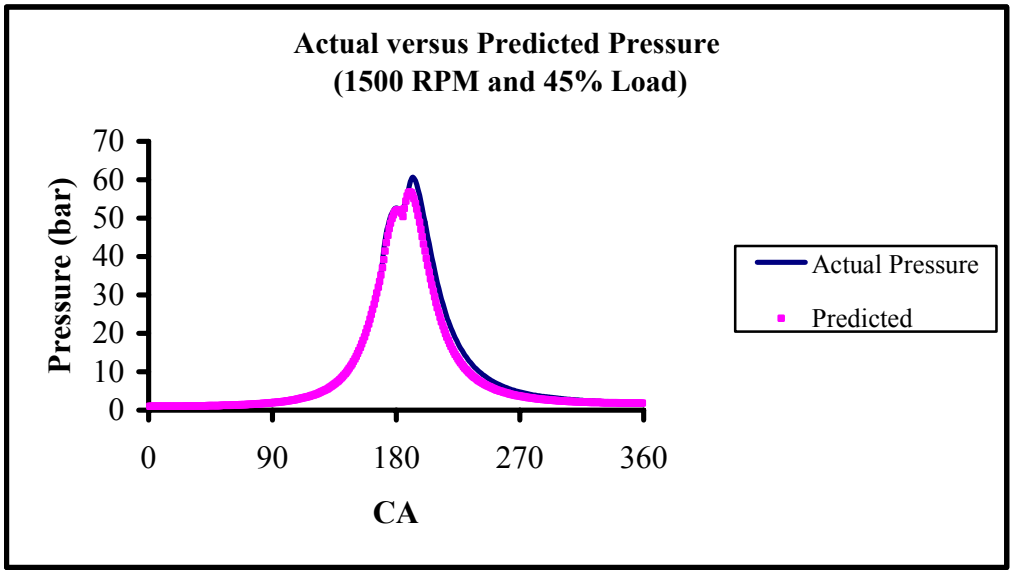

Figure 57. Actual versus Predicted Pressure (1500 RPM and 45% Load)

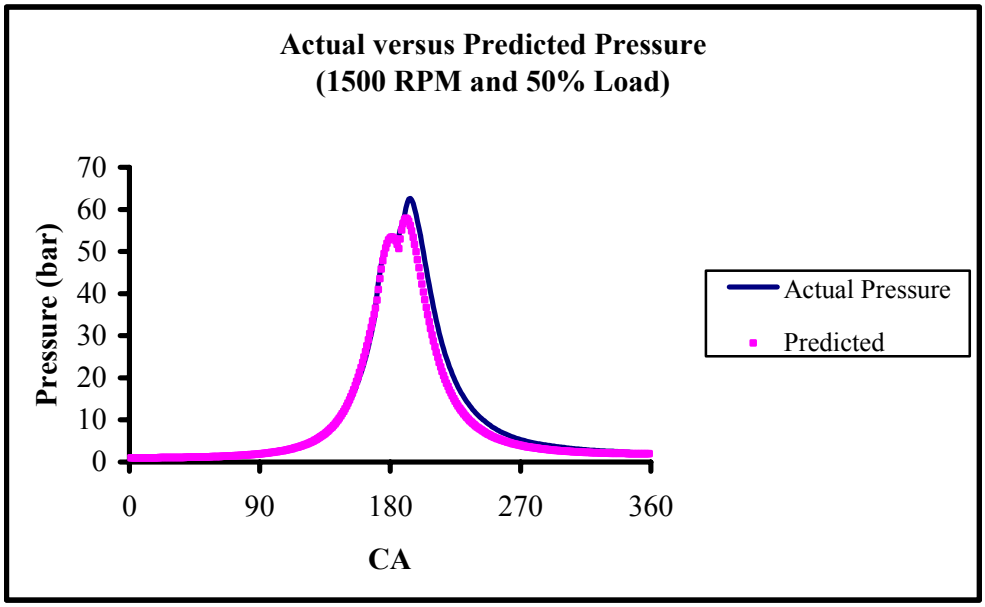

Figure 58. Actual versus Predicted Pressure (1500 RPM and 50% Load)

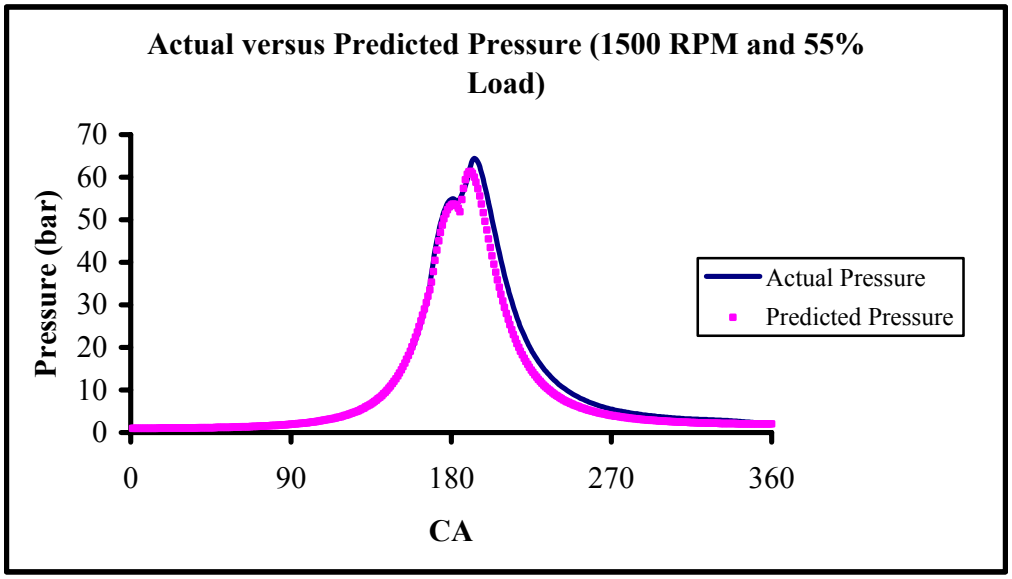

Figure 59. Actual versus Predicted Pressure (1500 RPM and 55% Load)

Figure 55 to 59 show that predicted pressures are close to the actual pressure.

Reccomendations

Data Acquisition: The cylinder pressure data was recorded in MAT file format. Readings for 100 cycles occupied 16.4 MB as compared to 400KB using binary file format. Suitable MATLAB program may be developed where data can be used in Binary file format.

LIST OF REFERENCES

References

1 PSA Peugeot Citroen Home Page. http://www.psa.fr/en_psaBB0026.html

2 MAN B&W Home Page. http://www.manbw.dk/

3 Heywood. J.B, 1988. "Fundamentals of Internal Combustion Engines", McGraw-Hill N.Y.

4 Lyn.W.T, 1978. "Optimization of Diesel Combustion Research", SAE Paper 780942

5 Eblen.E, Stumpp.G, 1978. "Beitrag des Einspritzsystems zur Verbesserung des Dieselmotors Bosch Techn. Berichte Band 6" Heft 2.

6 Stumpp and Ricco, 1996. "Common Rail-An attractive fuel injection system for passenger car DI Diesel Engines", SAE Paper 960870.

7 Stone. Richard, 1999."Introduction to Internal Combustion Engines", SAE.

8 Durnholz Manfred, Endres Helmut, and Frisse Peter, 1994."Pre-injection- A measure to optimize the emission behavior of DI-Diesel Engine", SAE Paper 940674.

9 Zhang, Long, 1999. "A study of pilot injection in a DI diesel engine", SAE paper 1999-01-3493.

10 Toshitaka Minami, Kouichi Takeuchi, and Naoki Shimazaki, 1995."Reduction of diesel engine NOx using pilot injection", SAE paper 950611.

11 Schommers Joachim, Duvinage Frank, Stotz Marco, Peters Arndt, Ellwanger Stefan, Koyanagi Katsuyoshi and Gilden Helmut, 2000. "Potential of common-rail injection systems for passenger car DI Diesel Engines", SAE Paper 2000-01-0944.

12 Patel Kirendra Palak, 2001. MS Thesis "Study of NOx and Loading of a Soot Filter

versus EGR for a 2.4L Diesel Engine".

13 Wlodarczyk Marek T., Poorman Tom, Arnold Jacob, Coleman Terry. 1999 "Long-Life Fiber-Optic Pressure Sensors for Harsh Environment Applications", 9th Trade Fair and Conference Sensor99.

14 Brunt.Michael.F.J and Gordon.Lucas.G, 1991. "The Effect of Crank Angle Resolution on Cylinder Pressure Analysis", SAE paper 910041.

15 Annand W.J.D, 1963. "Heat Transfer in the Cylinders of Reciprocating Internal Combustion Engine", Proc.I.Mech.E., Vol. 177.

16 Lancaster David R, Kreiger Roger B and Lienesch John H, 1975. "Measurement and Analysis of Engine Pressure Data", SAE Paper 750026.

17 Anderton D 1979. "Relation between Combustion System and Engine Noise", SAE Paper 790270.

18 Venkatesan C.Prasanna and Abraham John, 2000. "An Investigation of the Dependence of NO and Soot Emissions from a Diesel Engine on Heat Release Rate Characteristics, SAE Paper 2000-01-0509

19 Barba Christian, Burkhardt Christine, Boulouchos Konstantinos and Bargende Michael, 2000. "A Phenomenological Combustion Model for Heat Release Rate Prediction in High-Speed DI Diesel Engines with Common Rail Injection", SAE Paper 2000-01-2933.

APPENDIX

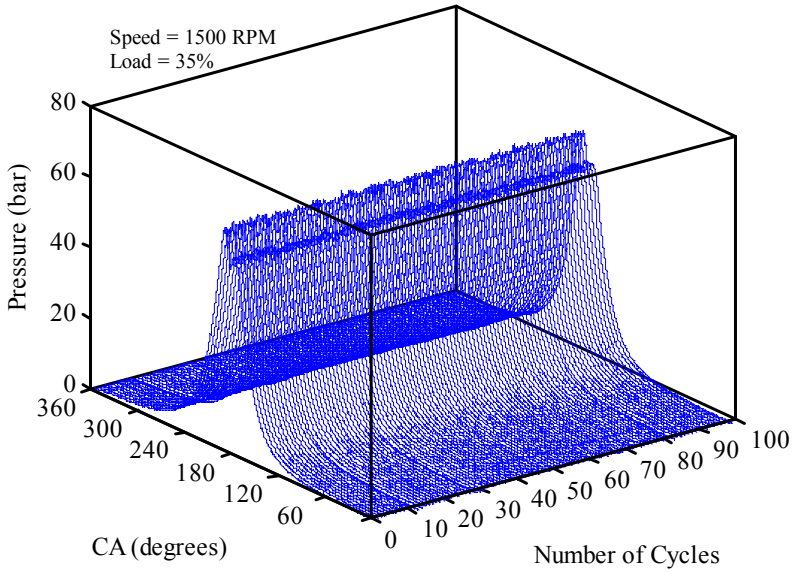

Figure 60. 3-D Plot showing Pressure versus Crank Angle for all the 100 cycles

Table 8. Cylinder Pressure Data Analysis (1500 RPM and 25%, 50% Load)

	1500 RPM and 25%load				1500 RPM and 50%load			
Cycle No.	Pmax (bar)	θ° CA ATDC	Work (Joules)	IMEP (bar)	Pmax (bar)	θ° CA ATDC	Work (Joules)	IMEP (bar)
1	49.3	11.2	185.4	3.9	62.0	12.6	337.6	7.1
2	50.2	10.6	179.1	3.8	62.4	12.2	339.8	7.1
3	49.7	10.9	179.2	3.8	62.1	12	333.3	7.0
4	49.3	11.6	173.6	3.6	62.5	12.6	331.0	6.9
5	50.1	10.3	193.3	4.0	61.9	12.5	341.0	7.1
6	50.3	10.2	180.5	3.8	62.9	12.4	352.4	7.4
7	49.2	10.8	186.5	3.9	61.6	12.1	338.0	7.1
8	49.8	10.3	183.7	3.8	62.2	12.7	334.7	7.0
9	49.2	11.8	178.5	3.7	61.0	12.4	327.5	6.9
10	48.9	10.9	187.3	3.9	62.4	12.5	324.3	6.8
11	49.6	11.3	172.7	3.6	61.6	13	339.6	7.1
12	49.6	10.9	192.8	4.0	61.9	12.2	341.0	7.1
13	50.2	10.5	183.1	3.8	61.8	12.6	340.8	7.1
14	49.7	12.2	190.3	4.0	62.5	12.5	338.3	7.1
15	49.5	10.4	172.2	3.6	62.4	12.6	333.8	7.0
16	49.1	10.5	179.4	3.8	62.4	12.3	340.1	7.1
17	49.1	10.2	177.3	3.7	61.8	12.6	332.1	7.0
18	49.1	10.7	186.1	3.9	62.0	12.1	337.6	7.1
19	49.3	11	169.4	3.5	61.9	12.5	336.6	7.1
20	48.9	10.5	182.9	3.8	62.2	12.6	338.4	7.1
21	49.0	10.5	180.2	3.8	61.3	12.7	334.9	7.0
22	49.5	11.6	181.6	3.8	62.5	12.6	351.4	7.4
23	49.4	10.8	177.0	3.7	62.1	12.6	334.2	7.0
24	49.2	11.5	182.5	3.8	62.2	13.2	340.8	7.1
25	50.1	10.8	186.0	3.9	62.1	12.4	328.9	6.9
26	49.6	11.1	186.4	3.9	62.7	12.4	341.6	7.2
27	49.0	10.2	151.1	3.2	61.6	12.8	331.1	6.9
28	49.0	11.8	190.0	4.0	61.8	13	333.7	7.0
29	49.4	10.9	178.2	3.7	61.9	12.3	336.4	7.0
30	49.9	10.3	171.4	3.6	60.9	12.9	336.9	7.1

Table 8 Continued								
	1500 RPM and 25%load				1500 RPM and 50%load			
Cycle No.	Pmax (bar)	θ° CA ATDC	Work (Joules)	IMEP (bar)	Pmax (bar)	θ° CA ATDC	Work (Joules)	IMEP (bar)
31	49.3	10.8	180.7	3.8	61.8	13.1	335.4	7.0
32	49.8	10.6	186.5	3.9	62.0	13.3	335.5	7.0
33	49.7	10.8	171.7	3.6	61.6	13.1	305.3	6.4
34	48.7	10.4	185.3	3.9	61.7	12.7	306.9	6.4
35	49.2	11.1	184.0	3.9	62.0	12.2	340.9	7.1
36	49.2	11	189.6	4.0	62.9	12.4	339.1	7.1
37	49.5	10.7	177.9	3.7	61.8	12.7	330.3	6.9
38	49.8	11	173.3	3.6	62.1	13.2	330.5	6.9
39	48.7	11.3	185.5	3.9	62.1	12.6	319.5	6.7
40	49.2	10.6	170.8	3.6	62.3	11.9	332.8	7.0
41	49.7	11	186.5	3.9	62.2	12.2	327.8	6.9
42	48.9	10.9	180.9	3.8	62.1	12.7	328.7	6.9
43	49.3	10.8	183.6	3.8	63.2	12.9	341.1	7.1
44	48.6	11.7	175.3	3.7	62.0	12.3	339.2	7.1
45	49.6	10.7	171.5	3.6	62.2	12.3	336.1	7.0
46	49.3	11.1	183.3	3.8	61.6	12.2	333.3	7.0
47	49.7	10.9	187.5	3.9	62.0	13	333.0	7.0
48	49.9	10.8	185.8	3.9	61.3	12.7	302.4	6.3
49	50.4	11.4	154.8	3.2	61.7	12.6	313.4	6.6
50	49.3	11.3	176.8	3.7	61.9	12.9	342.4	7.2
51	49.4	11	183.0	3.8	62.0	12.5	340.7	7.1
52	49.4	11	178.8	3.7	61.9	12.7	329.3	6.9
53	49.3	11.3	182.0	3.8	62.7	12.6	340.8	7.1
54	49.9	10.8	175.6	3.7	61.8	12.3	333.6	7.0
55	50.3	11.2	179.8	3.8	62.7	12.6	340.9	7.1
56	49.4	10.7	178.1	3.7	61.8	12.6	311.8	6.5
57	50.0	10.4	187.7	3.9	61.5	12.5	337.2	7.1
58	48.3	10.7	165.8	3.5	62.4	12.6	342.4	7.2
59	49.5	11.2	152.7	3.2	62.3	13	340.7	7.1
60	49.3	11.2	178.5	3.7	61.3	11.9	327.6	6.9

Table 8 Continued								
	1500 RPM and 25%load				1500 RPM and 50%load			
Cycle No.	Pmax (bar)	θ° CA ATDC	Work (Joules)	IMEP (bar)	Pmax (bar)	θ° CA ATDC	Work (Joules)	IMEP (bar)
61	49.6	11.3	177.5	3.7	62.8	12.5	332.4	7.0
62	49.2	11	182.5	3.8	61.5	12.7	325.6	6.8
63	49.1	11.1	186.8	3.9	61.5	12.6	330.5	6.9
64	48.7	10.6	162.2	3.4	61.9	12.9	334.3	7.0
65	49.9	10.9	190.1	4.0	61.6	12.4	332.6	7.0
66	48.9	10.9	178.2	3.7	61.3	12.9	334.1	7.0
67	50.0	10.8	162.7	3.4	62.2	12.3	344.2	7.2
68	48.9	10.9	173.7	3.6	61.5	12.4	311.0	6.5
69	49.3	11.4	182.6	3.8	62.5	12.3	340.7	7.1
70	49.2	11.3	174.5	3.7	62.0	12.5	338.8	7.1
71	48.9	11.6	187.3	3.9	61.9	12.4	340.2	7.1
72	49.8	10.6	146.5	3.1	61.8	12.9	337.4	7.1
73	49.5	10.5	170.2	3.6	62.4	12.3	338.0	7.1
74	49.7	10.6	154.2	3.2	61.4	12.8	333.4	7.0
75	49.8	10.6	164.4	3.4	61.7	12.3	337.3	7.1
76	50.2	10.8	183.7	3.8	61.8	12.1	335.9	7.0
77	48.8	10.4	190.5	4.0	62.0	12	322.8	6.8
78	49.4	10.3	179.0	3.7	61.4	13	314.8	6.6
79	49.1	10.6	184.2	3.9	62.8	12.6	343.2	7.2
80	49.9	10.6	184.1	3.9	62.0	12	333.4	7.0
81	48.8	10.6	187.3	3.9	62.1	12.7	335.0	7.0
82	49.6	11	178.2	3.7	61.8	12.7	329.1	6.9
83	49.1	11	145.3	3.0	61.6	12.3	336.4	7.0
84	51.0	10.6	177.0	3.7	62.8	13.1	338.0	7.1
85	49.3	11	175.6	3.7	62.3	12.7	344.8	7.2
86	49.6	11.4	182.3	3.8	62.2	12.6	339.1	7.1
87	50.0	10.7	174.9	3.7	62.2	13.2	342.3	7.2
88	50.0	11.1	183.3	3.8	61.8	12.3	338.5	7.1
89	49.1	10.4	156.7	3.3	61.8	12.8	333.1	7.0
90	49.0	11	190.3	4.0	62.5	12.6	342.9	7.2

Table 8 Continued								
	1500 RPM and 25%load				1500 RPM and 50%load			
Cycle No.	Pmax (bar)	θ° CA ATDC	Work (Joules)	IMEP (bar)	Pmax (bar)	θ° CA ATDC	Work (Joules)	IMEP (bar)
91	48.6	10.7	182.8	3.8	62.0	12.3	337.1	7.1
92	49.4	10.8	180.6	3.8	62.2	12.4	341.9	7.2
93	49.7	10.8	178.6	3.7	62.1	12.6	331.1	6.9
94	49.7	10.2	186.1	3.9	61.9	12.8	333.4	7.0
95	50.0	10.6	177.6	3.7	61.9	12.9	334.5	7.0
96	49.9	10.6	190.9	4.0	62.1	12.2	332.5	7.0
97	49.1	11.1	176.6	3.7	61.8	12.7	335.9	7.0
98	49.5	10.8	179.3	3.8	62.7	13.1	342.4	7.2
99	49.3	10.6	176.9	3.7	62.3	13	340.3	7.1
100	49.6	10.6	185.3	3.9				

Table 9. Cylinder Pressure Data Analysis (1800 RPM and 25%, 50% Load)								
	1800 RPM and 30%load				1800 RPM and 50% load			
Cycle No.	Pmax (bar)	θ°CA ATDC	Work (Joules)	IMEP (bar)	Pmax (bar)	θ°CA ATDC	Work (Joules)	IMEP (bar)
1	60.8	12.7	238.5	5.0	76.2	12.9	375.5	7.9
2	61.4	13.1	243.4	5.1	71.2	13.1	330.4	6.9
3	61.0	12.5	240.3	5.0	72.2	12.9	360.6	7.6
4	61.7	12.9	244.2	5.1	71.0	14.8	380.2	8.0
5	60.5	13.1	240.6	5.0	70.3	14.8	384.1	8.0
6	62.1	13.0	238.3	5.0	69.7	13.7	376.6	7.9
7	60.8	12.4	237.7	5.0	70.4	14.5	385.0	8.1
8	60.9	11.9	238.6	5.0	70.3	14.5	376.3	7.9
9	60.8	13.0	241.7	5.1	71.2	14.5	391.8	8.2
10	60.5	12.9	240.8	5.0	70.0	14.5	380.6	8.0
11	60.7	12.7	233.7	4.9	71.2	14.4	386.3	8.1
12	60.8	12.5	244.6	5.1	71.2	14.1	378.1	7.9
13	62.1	13.4	234.7	4.9	72.3	14.1	382.2	8.0
14	60.9	12.4	238.5	5.0	71.5	13.7	381.6	8.0
15	61.6	13.5	240.6	5.0	71.0	14.6	392.6	8.2
16	60.7	12.5	232.8	4.9	70.7	13.4	377.7	7.9
17	60.0	13.7	238.8	5.0	70.6	14.4	387.9	8.1
18	61.1	13.0	245.2	5.1	69.8	14.9	383.6	8.0
19	60.7	12.9	237.9	5.0	69.0	14.7	383.6	8.0
20	62.6	12.1	229.5	4.8	69.8	14.8	379.1	7.9
21	60.1	13.1	241.3	5.1	71.2	14.6	390.7	8.2
22	61.0	12.6	233.3	4.9	71.4	13.2	380.8	8.0
23	60.4	11.9	237.9	5.0	73.2	14.4	391.8	8.2
24	60.7	12.7	229.7	4.8	73.0	13.5	376.3	7.9
25	61.2	13.1	241.7	5.1	73.9	14.4	389.6	8.2
26	62.0	12.1	240.9	5.0	72.6	14.1	384.3	8.1
27	62.0	12.8	243.8	5.1	72.7	14.0	394.1	8.3
28	60.5	12.6	239.5	5.0	71.6	14.4	383.0	8.0
29	60.9	12.5	240.8	5.0	73.0	13.7	379.8	8.0
30	60.4	13.0	230.7	4.8	73.3	14.1	388.8	8.1

Table 9 Continued

	1800 RPM and 30%load				1800 RPM and 50% load			
Cycle No.	Pmax (bar)	θ°CA ATDC	Work (Joules)	IMEP (bar)	Pmax (bar)	θ°CA ATDC	Work (Joules)	IMEP (bar)
31	61.0	11.9	236.1	4.9	72.4	14.1	389.1	8.1
32	59.5	13.2	235.7	4.9	71.2	14.8	374.9	7.9
33	60.0	12.9	241.4	5.1	72.2	14.6	378.9	7.9
34	60.7	13.1	239.6	5.0	70.4	14.6	382.0	8.0
35	61.1	12.7	243.3	5.1	69.8	14.7	377.5	7.9
36	60.6	13.1	229.8	4.8	69.3	15.9	389.6	8.2
37	60.0	12.9	234.9	4.9	68.0	14.8	376.7	7.9
38	60.4	13.2	233.5	4.9	67.2	14.9	386.1	8.1
39	60.8	11.8	237.7	5.0	68.3	15.3	377.4	7.9
40	61.4	12.7	227.7	4.8	68.3	14.7	387.9	8.1
41	61.7	12.6	241.6	5.1	68.4	14.3	380.6	8.0
42	60.7	13.1	237.3	5.0	70.9	14.4	393.5	8.2
43	60.7	12.7	243.8	5.1	72.0	14.0	385.7	8.1
44	60.5	12.1	229.3	4.8	72.2	14.2	393.2	8.2
45	61.5	12.6	243.1	5.1	72.3	13.1	370.1	7.8
46	61.6	13.9	234.4	4.9	72.3	13.5	380.1	8.0
47	61.4	13.8	239.5	5.0	71.2	13.3	360.7	7.6
48	61.8	12.5	235.6	4.9	70.7	12.6	345.0	7.2
49	60.0	12.9	236.9	5.0	71.7	13.6	366.4	7.7
50	60.3	12.1	231.5	4.8	73.4	14.0	365.0	7.6
51	60.1	12.3	229.4	4.8	72.4	14.7	373.4	7.8
52	60.3	12.1	228.5	4.8	71.9	13.5	377.9	7.9
53	60.4	13.0	233.3	4.9	71.7	13.9	377.1	7.9
54	62.0	13.6	233.7	4.9	71.5	13.6	383.0	8.0
55	61.2	12.5	236.6	5.0	70.8	14.6	381.9	8.0
56	61.1	12.0	241.3	5.1	70.5	13.3	387.2	8.1
57	63.1	13.0	241.9	5.1	71.7	13.7	378.2	7.9
58	60.7	12.6	245.2	5.1	72.3	14.1	389.9	8.2
59	61.7	12.2	244.2	5.1	70.3	14.2	380.1	8.0
60	61.3	11.5	246.6	5.2	71.2	14.3	389.7	8.2

Table 9 Continued

	1800 RPM and 30%load				1800 RPM and 50% load			
Cycle No.	Pmax (bar)	θ°CA ATDC	Work (Joules)	IMEP (bar)	Pmax (bar)	θ°CA ATDC	Work (Joules)	IMEP (bar)
61	61.6	12.8	243.3	5.1	70.6	13.0	373.5	7.8
62	61.4	13.3	240.1	5.0	68.9	15.1	378.2	7.9
63	60.7	12.9	238.8	5.0	68.9	14.9	380.5	8.0
64	61.3	12.2	238.1	5.0	67.5	14.8	381.1	8.0
65	60.7	12.5	235.2	4.9	66.3	15.6	381.5	8.0
66	61.0	12.7	240.4	5.0	65.0	14.9	384.0	8.0
67	60.8	13.6	233.4	4.9	63.7	16.1	387.5	8.1
68	61.7	12.4	242.2	5.1	63.4	15.9	388.2	8.1
69	60.4	11.6	233.4	4.9	66.2	14.9	382.6	8.0
70	61.5	12.1	242.1	5.1	68.0	14.7	396.8	8.3
71	60.8	11.5	233.2	4.9	71.7	14.3	387.2	8.1
72	59.6	13.8	239.9	5.0	72.8	13.7	394.2	8.3
73	60.1	12.8	236.1	4.9	72.9	13.6	376.0	7.9
74	60.1	12.8	241.4	5.1	72.9	13.4	374.0	7.8
75	61.4	11.6	236.7	5.0	72.4	13.3	337.8	7.1
76	60.9	11.9	236.3	4.9	71.3	12.6	338.3	7.1
77	59.7	13.1	232.6	4.9	75.5	12.6	359.0	7.5
78	61.7	12.4	245.2	5.1	74.0	14.5	369.3	7.7
79	61.5	12.4	232.1	4.9	74.3	14.1	380.3	8.0
80	61.3	13.3	238.2	5.0	71.1	13.3	361.1	7.6
81	62.0	11.5	236.2	4.9	69.9	14.5	371.3	7.8
82	61.8	11.9	241.4	5.1	71.9	13.9	381.1	8.0
83	60.3	11.8	238.9	5.0	70.5	14.3	379.6	8.0
84	60.9	12.6	242.0	5.1	71.2	14.3	383.5	8.0
85	60.6	12.7	230.5	4.8	69.9	14.1	389.0	8.1
86	61.2	13.6	238.6	5.0	70.5	14.4	371.1	7.8
87	60.8	12.8	235.6	4.9	71.8	14.4	385.8	8.1
88	60.9	13.3	236.8	5.0	72.3	14.7	382.9	8.0
89	61.4	12.2	237.7	5.0	72.8	14.1	389.5	8.2
90	60.8	12.6	238.8	5.0	73.4	13.6	385.7	8.1

Table 9 Continued								
	1800 RPM and 30%load				1800 RPM and 50% load			
Cycle No.	Pmax (bar)	θ°CA ATDC	Work (Joules)	IMEP (bar)	Pmax (bar)	θ°CA ATDC	Work (Joules)	IMEP (bar)
91	61.1	12.4	232.0	4.9	72.6	13.5	388.3	8.1
92	60.1	12.9	239.4	5.0	70.9	14.2	383.9	8.0
93	60.1	13.0	240.0	5.0	71.7	14.6	385.0	8.1
94	60.2	13.0	239.7	5.0	70.2	14.2	374.4	7.8
95	60.8	12.7	236.1	4.9	70.6	14.6	380.9	8.0
96	59.9	12.5	242.7	5.1	68.4	14.8	375.6	7.9
97	62.3	12.0	236.1	4.9	67.5	14.9	391.8	8.2
98	60.9	11.7	235.1	4.9	68.4	15.1	375.3	7.9
99	60.1	12.0	241.2	5.1	69.1	14.7	395.8	8.3
100	60.6	12.8	240.5	5.0	69.3	13.6	374.4	7.8

Matlab Programs Used

Program 1

%the.m%

```
%% this matlab file plots the pressure v/s crankangle curve from
%% the Data recorded by Wavebook in MAT format.

A=input ('Enter A');              % note enter "A" - case sensitive
a=A(:,2);                         % value of all pressures
a=a-.5;                           % 0.5V=0psi
a=a*(1000/(1.51*14.5038));        % conversion from mv to bar.14.5038 is for
                                  % conversion from psi to bar.1.51mv/psi
b=A(:,3);                         % value of all index
c=A(:,1);                         % value of all fuel injection

%%%sub-routine to align TDC%%%
x=1:14400;
p1=a(1:14400);
plot(x,p1)              % TDC is visually aligned.
shift=input('Enter value to align TDC');
%TDC is aligned in such a way that first peak in cylinder pressure curve is at TDC
%%% sub-routine to align TDC ends.%%%


%%% sub-routine for pressure matrix.%%%
 [m,n]=size(a);
j=m/7200;
ind=zeros(3601,1);   % Initialisation Matrix
for i=1:j;
   if (shift+7200*(i-1)+1800<m)
   pre=a(shift+7200*(i-1)-1800:shift+7200*(i-1)+1800);   % recording of 1800 points
   ind=cat(2,ind,pre);                                    % on either side of TDC
end
end
p=ind(:,2:end);
p=p';
%%% sub-routine to form pressure matrix ends%%%

%%% sub-routine to ensure that p always has positive value%%%
[m,n]=size(p);
for i=1:m;
   mini=min(p(i,:));
```

```
   p(i,:)=p(i,:)-1*mini+.001;
end
%%% sub routine ends %%%

pmean=mean(p);            % Calculation of pmean
x=1:3601;
plot(x*.1,pmean)
pr=p';
[pmax,theta]=max(pr);   % Pmax and it's position


%%% Injection data matrix%%%
ind=zeros(3601,1);
[m,n]=size(c);
j=m/7200;
for i=1:j;
   if (shift+7200*(i-1)+1800<m)
   preinj=c(shift+7200*(i-1)-1800:shift+7200*(i-1)+1800);
   ind=cat(2,ind,preinj);
end
end
inj=ind(:,2:end);
inj=inj';
```

Program 2

```
%%% Program to calculate work done and IMEP for each cycle%%%


p=input('enter value of pressure'); % Enter "p".
                                    % "p"= pressure matrix obtained by th.m


% Calculation of Volume as a function of Crank Angle
% Cylinder Bore=82mm
% Stroke=90.4mm
% Length of Connecting Rod = 150
% 11.0131 = (150/45.2)^2
vd=(pi*82^2*90.4)/4;
vol=0;
for theta=180:.1:540
   a=2.2166-.5*(cos(pi*theta/180)+sqrt(11.0131-(sin(pi*theta/180)^2))); %%% refer
                                                                %www.colostate.edu
   v=vd*a*0.000000001;
   vol=cat(2,vol,v);
end
vol=vol(:,2:end);

%%%  Calculation Ends %%%
dvol=diff(vol);             % Volume change for every crankangle
[m,k]=size(p);
n=1:m;
plot(vol,p(n,:),'.')                % Plotting P-V diagram for all cycles
p=p(:,2:end);                       % Note Pressure matrix Changed
work=p*dvol'*100000                 % Evaluation of work done/cycle
mep=work/(max(vol)-min(vol))   % IMEP evaluation
```

Program 3

```
%% this program takes Pressure matrix formed using "th.m" and averaged,
%% smoothed pressure data is returned

p=input('value of p');  % enter "p" where is "p" is the
                        % pressure matrix formed by th.m

pavg=mean(p);          % pressure data averaged

%%% sub-routine for smoothing pressure data%%%

for j=5:3597;
psmo(j-4)=((-21*pavg(j-4)+14*pavg(j-3)+39*pavg(j-2)+54*pavg(j-
1)+59*pavg(j)+54*pavg(j+1)+39*pavg(j+2)+14*pavg(j+3)-21*pavg(j+4)))/231;
end

%%% sub-routine ends%%%

%%% average of 10 points taken.%%%
[m,n]=size(psmo);

i=0;
for j=0:10:n-10
   n1=psmo(j+1:j+10);
   i=[i,mean(n1)];
end
pdata=i(2:end);
dp=diff(pdata);
[i,j]=size(dp);
x=1:j;
plot(x,dp)

 %%% Subroutine to ensure that intake pressure is 1 Atm%%%
if pdata(1)<1
   add=1-pdata(1);
   pdata=pdata+add;
end
% %% Subroutine ends%%%
```

Program 4

```
%%%Heat release analysis is done using this file%%%
%%Use pdata as the input value for pressure.pdata is evaluated using file avgdata%%%
%%%the pressure data is averaged,smoothed and average of 10 points is taken%%%

pheat=input('enter value of p "hint=enter pdata"');  %%% enter pdata as input

%%% Volume versus CA calculations repeated%%%
vol=0;
vd=(pi*82^2*90.4)/4;
for theta=181:1:540
   a=2.2166-.5*(cos(pi*theta/180)+sqrt(11.0131-(sin(pi*theta/180)^2)));
   v=vd*a*0.000000001;
   vol=cat(2,vol,v);
end
vol=vol(:,2:end);
dvol=diff(vol);

%%%Sub-routine Ends%%%

%%% specific volume calculation%%%
vol1=0;
%% Derivation of Initial Specific Volume%%%
% assumed intial temperature= 300K
% assumed initial Pressure= 100,000 N/m2
% Initial specific volume= 287*300/100,000 =0.861 m3/Kg

spv=0.861;
for theta=180:1:540
   spvo=0.861*((1/18.45)+(17.45)/(2*18.45)*(1-(cos(pi*theta/180))));
   vol1=cat(2,vol1,spvo);
end
spvol=vol1(:,2:end);
[i,j]=size(pdata);
spvol=spvol(1:j);   % Ensure that specific volume matrix and pressure matrix
% are of same size
%%% specific volume calculation ends.%%%

%%%  Surface Area Calculations%%%
for theta= 180:1:540
   area(theta-179)=pi*(0.082)^2*0.5+pi*(0.082)*(0.0904)*0.5*(1-cos((theta)*pi/180));
end
area=area(1:j);
```

```
%%% Area Caluculations End%%%
%%% All constants evaluated%%%

for k=1:j
   t(k)=pdata(k)*spvol(k)*100000/287;
   gamma(k)=1.338-6*0.00001*t(k)+0.00000001*t(k)*t(k);
   cvr(k)=1/(gamma(k)-1); %%%%% value of Cv/R actual value instead of
approximation Cv/R=3.5
   cp(k)=241.1/(1-(1/gamma(k)));
   mu(k)=4.702*(1e-07)*(t(k))^(0.645);
   lambda(k)=cp(k)*mu(k)/0.7;
   reynold(k)=4.52*0.082/(spvol(k)*mu(k));
   h(k)=.35*lambda(k)*(reynold(k))^0.7/0.082+.576*5.67*(1e-08)*(((t(k))^4-
400^4)/(t(k)-400));
   qwall_loss(k)=h(k)*area(k)*(t(k)-400)/25;     % Heat Loss is in Watts to convert to
                                                 % heat loss/cycle
end                                  % divide by 25.Engine RPM=1500. therefore
                                     % 1cycle=60/1500 secs

%%% Constant Evaluation Ends%%%


%%% Sub-routine for rate of heat-release.%%%
%%% first term evaluation%%
%%% the pressure data is averaged,smoothed and averaged of 10 points is taken.%%%

%%%%  first term of total heat released.%%%
pvinit=zeros(1,359);
[m,n]=size(pheat);
for i=1:n;
   qfirst(i)=cvr(i)*(100000*pheat(i)*vol(i)-2.74);
   pv(i)=100000*pheat(i)*dvol(i);
end

%%% First term calculation ends%%%

%%% second term of total heat released.%%%
for i=1:n;
   qsecond(i)=sum(pv(1:i));
end

%%% Second term calculation ends%%%
q=qfirst+qsecond;  % Total Sum without heat loss to walls
```

```
[i,j]=size(q);
x=1:j;
qtotal=qwall_loss+q; % Total Sum with heat loss to walls
x=1:359;figure(1);plot(x,q/max(qtotal),x,qtotal/max(qtotal))
q=q/max(qtotal);
qth=diff(q);
[m,n]=size(qth);
x=1:n;
figure(2); plot(x,qth
```

Vita

M.Rajkumar was born in Madurai, India on May 9, 1973. He was raised in New Delhi, India. He graduated from Delhi College of Engineering in 1995. From there, he went to Lurgi India Company Private Limited where he briefly worked for a period of 3 months and then later moved on to Maruti Udyog Limited, India in October 1995. He continued working there until July 2000. He joined University of Tennessee, Knoxville in Aug 2000 and graduated in Summer 2002.